7 Tectonic Geomorphology, Quaternary Chronology, and Paleoseismicity

E. A. Keller[1] and T. K. Rockwell[2]

Introduction

Tectonic geomorphology, defined as the application of geomorphology to tectonic problems, includes the study of landform assemblages and landscape evolution as well as development of process-response models for areas and regions affected by recent tectonic activity. Of particular interest in the study of the earthquake hazard for a particular area are problems associated with deriving rates of faulting and determination of paleoseismicity (study of prehistoric earthquakes) for the late Pleistocene and Holocene. Tectonic geomorphology is a relatively new branch of applied geomorphology, the study of which requires understanding of a number of disciplines other than geomorphology including structural geology, Quaternary stratigraphy, pedology and geochemistry as it relates to weathering-soils and absolute dating techniques.

Study of tectonic geomorphology requires more than a modest acquaintance with principles of landscape evolution mixed with an understanding of geomorphic processes. A relationship or framework for studying landscape evolution and process (Gregory 1978) is that the landscape, landform assemblage, or landform is a function of geomorphic process (eg. weathering, fluvial, tectonic) and earth materials (eg. soil, water, rock) integrated over time. This relationship, although not an equation, may be expressed as:

$$F = f(P, M)\,dt \qquad (1)$$

where F is the form of landscape or landform; f denotes "a function of"; P is geomorphic processes or process; M is earth materials broadly defined to include texture, composition and geologic structure; and dt represents change in time. This relationship provides a simple way of summarizing several approaches or levels of geomorphic inquiry (Gregory 1978):

Level one: The study of elements of the relationship. That is, investigation of the form of the landscape, geomorphic process, or earth materials independent of each other and of time.

Level two: Obtaining relationships between the independent variables (geomorphic process and earth materials) and the dependent variable (the form of the landscape or landform) independent of time.

1 Department of Geological Sciences, University of California, Santa Barbara, CA 93106, USA
2 Department of Geological Sciences, California State University, San Diego, CA 92182, USA

Developments and Applications of Geomorphology
Edited by J. E. Costa and P. J. Fleisher

Level three: Evaluation of relations between the variables (landform, geomorphic process and earth materials) over time. In mathematical terms this requires integrating the relationship, geomorphically it requires the study of landscape evolution.

When results from the above three levels of geomorphic inquiry are applied to the study of environmental problems we enter the domain of applied geomorphology. Problems in tectonic geomorphology, such as the study of the paleoseismicity of an area or site, often require working at all three levels, but in particular involve evaluation of landforms and associated materials (eg. soils, deposits, fractures in rocks) produced by tectonic processes during the late Pleistocene and Holocene.

The significant application of tectonic geomorphology to paleoseismicity involves determining both chronology of earth materials and rates of tectonic processes for a particular study site. Recognizing this, the objectives of this paper are: 1. to discuss Quaternary chronology, methods of relative and absolute dating, and time scales useful in tectonic geomorphology; 2. to discuss geomorphic indicators of tectonic activity and paleoseismicity; and 3. to discuss neotectonics and the earthquake hazard.

Quaternary Chronology

The Quaternary period includes the Pleistocene and Holocene epochs, roughly the last two million years of geologic time. This time period is particularly important to engineering geology, tectonic geomorphology and neotectonic studies because most presently active geologic structures have either developed during or continued to develop over this time period, and study of these features may indicate their future behavior. This is especially true in studying active faulting and developing estimates of probable future seismicity. Thus, it is important to establish a well defined chronology based as much as possible on absolute dating of sediments involved in active faulting and folding.

Methods of dating Quaternary deposits will be discussed first with the intent of introducing several of the various available techniques and their usefulness rather than attempting to explain in depth the intricacies of the individual methods. The Quaternary time scale will then be outlined based upon some of the dating techniques.

Dating Techniques

There are principally three general categories of dating used in Quaternary studies; direct dating by radiometric or chemical methods, dating by correlation to deposits of known age, and relative dating methods (Coleman and Pierce 1977). Direct dating techniques involving radioactive decay include ^{14}C, uranium-series, fission track, potassium-argon, and lead isotope methods. The principal chemical methods include amino acid racemization, obsidian hydration, heavy mineral etching, surface weathering, and soil development. Dating by correlation also includes soil development and stratigraphy, as well as tephrachronology, dendrochronology and paleomagnetism. There is some overlap between absolute, relative and correlative applications among some methods, especially those involving chemical weathering and diagenesis rates which vary from place-to-place and under different climatic and temperature conditions such as soil development, mineral etching, weathering phenomenon and amino acid diagenesis. Commonly, more than one method is employed which collectively provide a more reliable age estimate. Table 1 summarizes some of the dating techniques in terms of effective and possible age ranges.

Table 1. Effective (solid line) and possible (dashed line) age ranges of techniques for dating Quaternary deposits and geologic materials. Included is the Quaternary timescale; note the scale's non-linearity. Compiled and modified from Bowen (1978) and Packer et al. (1975)

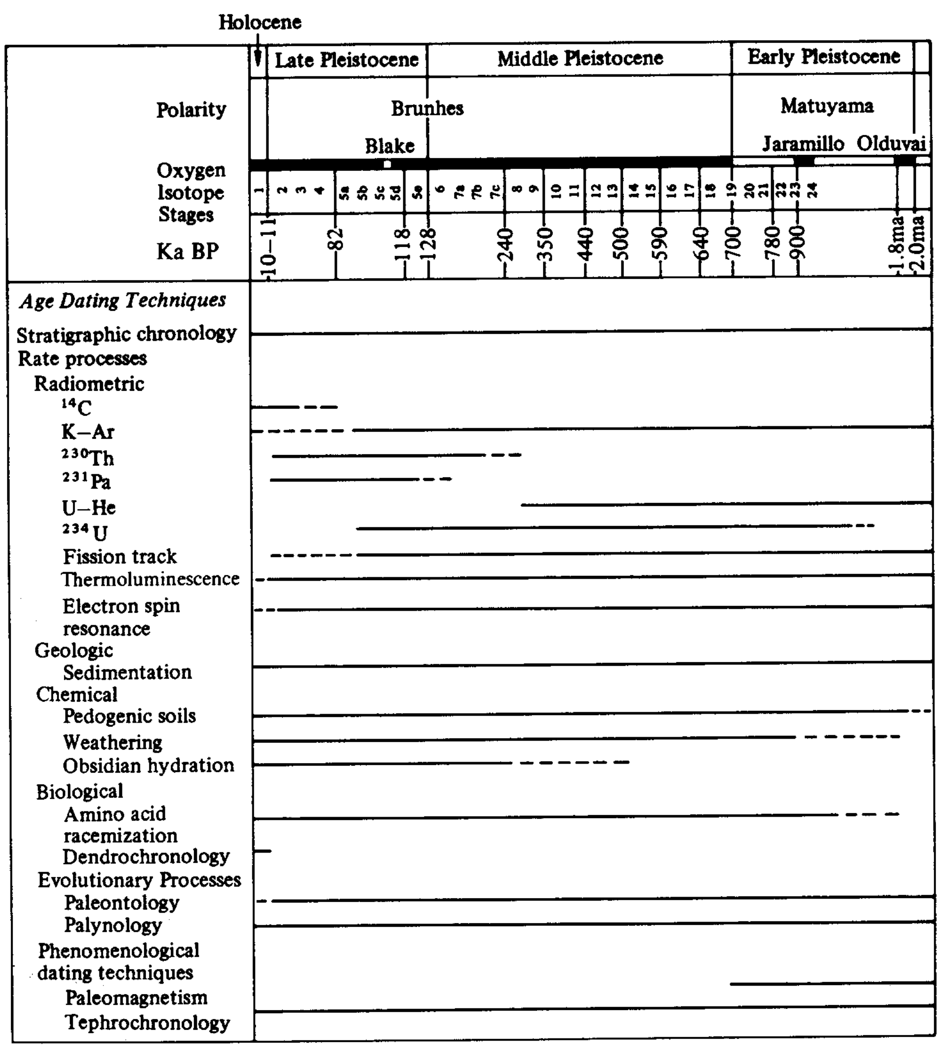

Carbon-14

The ^{14}C dating technique is one of the older and most reliable methods for dating late Pleistocene and Holocene deposits providing certain guidelines are followed. The ^{14}C method, pioneered by W.F. Libby in the 1950's, is based upon the determination of the ratio of ^{14}C to ^{12}C in carbonaceous substances. This method is generally good to about 40×10^3 years B.P. by standard counting techniques but may be extended to nearly 100×10^3 years B.P. when the $^{14}C/^{12}C$ ratio is determined with an accelerator. ^{14}C is produced in the upper atmosphere, oxidized and then mixed through the atmosphere near the earth's surface where it is taken up by plants through photosynthesis or by other organisms through the food chain. The ratio of ^{14}C to ^{12}C in the atmosphere is considered to be nearly constant although it has varied through time (Yang and Fairhall 1972). Similarly, the $^{14}C/^{12}C$ ratio may be different than that in the atmosphere for different biospheres such as the oceans, lakes, and rivers. This may cause a ^{14}C age to deviate from its real age by a considerable amount as discussed below. Because of these and other problems and constraints, some material is more suitable for dating than others.

Charcoal is essentially inert; once burned, carbon atoms will not mobilize and replace other carbon atoms. However, contamination may occur by adding dead carbon in the form of $CaCO_3$ or recent carbon in the form of fulvic and humic acid from plants. Thus, it is necessary to pre-treat all samples, if possible, with dilute HCl and NaOH which remove these contaminants, especially if the samples were recovered within the weathering profile of a soil.

Dendrochronologic and varve-chronologic calibration indicates that the present concentration of ^{14}C in the atmosphere has not always remained constant and dates determined for samples less than about 10,000 years must be corrected (Yang and Fairhall 1972; Stuiver 1982; Klein et al. 1982). For a complete set of correction tables, refer to Klein et al. (1982). Additionally, different species selectively absorb more ^{14}C than others (Olsson and Osadebe 1974).

Peat and wood also tend to be reliable for ^{14}C dating although there is some chance of contamination if the sample is in an oxidizing environment and is being carbonized. In this case, care must be taken to sample as much of the original material as possible. Peat, however, may have been derived from plants grown in an aquatic environment and the original $^{14}C/^{12}C$ ratio may have been different in that particular reservoir than in the atmosphere.

Shells have proven unreliable in many cases for similar reasons to peat; the $^{14}C/^{12}C$ ratio is seldom identical in lakes and oceans as that in the atmosphere. Dead carbon derived from limestone may be used by the organisms which in turn yield dates which appear older than their real value and must be corrected (Mangerud and Gulliksen 1975). Shells also tend to act as an open system. Most shell is composed of aragonite, an unstable form of $CaCO_3$, and tends to recrystallize to calcite with time. During recrystallization, carbon atoms may be replaced by older or younger ones dependent on the dominant type in solution. Thus, finite dates have been obtained on very old shell material (Olsson 1974) (see Table 2).

To avoid some problems with dating shell, the outer layer is commonly dissolved away with dilute HCl. This is intended to remove that part which has recrystallized or may have acted as an open system and exchanged carbon. Nevertheless, shell

Table 2. Effect of
(from Polach and (

(A) True sample Age (years)
5,000
10,000
20,000
30,000
100,000

(B) True sample Age (years)
500
5,000
10,000
20,000

dates are seldor
problematic in t
it is sometimes r
termination.

Uranium Series

Uranium series
to about 250 × 1
are used, ^{238}U ;
^{238}U decays to
= 7.52 × 10^4 yea
years. An equili
Organisms may
create an imba
portions of the ;
the original pro
The second assı
different U-serie
Dating of fc
Chappell 1974;
control on not
hence, periods c
Uranium-se
and deposits bı

Table 2. Effect of contamination by modern (A) and old (B) carbon on the true sample age (from Polach and Golson, 1966)

(A)

True sample Age (years)	Apparent age after contamination by modern carbon (years)			
	1%	5%	20%	50%
5,000	4,950	4,650	3,700	2,100
10,000	9,800	9,000	6,800	3,600
20,000	19,100	16,500	10,600	5,000
30,000	27,200	21,000	12,200	5,400
100,000	37,000	–	–	–

(B)

True sample Age (years)	Apparent age after contamination by old carbon (years)			
	5%	10%	20%	50%
500	900	1,300	2,200	6,000
5,000	5,400	5,800	6,700	10,500
10,000	10,400	10,800	11,700	15,500
20,000	20,400	20,800	21,700	25,500

dates are seldom reliable much beyond 30×10^3 years B.P. ^{14}C dating of bone is problematic in that it is primarily $CaPO_4$ and does not contain much carbon. Thus, it is sometimes necessary to consume large quantities of bone for a singular age determination.

Uranium Series

Uranium series techniques have been used to date a wide variety of substances back to about 250×10^3 years, some with better results than others. Two uranium nuclides are used, ^{238}U and ^{235}U, which decay to relatively short lived daughter products. ^{238}U decays to ^{234}U ($t^{1/2} = 2.5 \times 10^5$ years) which in turn decays to ^{230}Th ($t^{1/2} = 7.52 \times 10^4$ years). Similarly, ^{235}U decays to ^{231}Pa which has a half-life of 3.24×10^4 years. An equilibrium exists between the parent nuclide and the daughter products. Organisms may only absorb uranium during life or shortly after death and thereby create an imbalance which begins to equilibrate. By measuring the relative proportions of the parent and daughter nuclides, the age may be determined assuming the original proportions are known and the sample has remained a closed system. The second assumption is usually the hardest to prove but may be inferred if the different U-series ages are concordant.

Dating of fossil coral reefs has proven the most successful (Bloom et al. 1974; Chappell 1974; Broecker et al. 1968; Thurber et al. 1965) and has provided excellent control on not only the timing but the level of high and low sea level stands and hence, periods of glaciation.

Uranium-series dating of mollusk shell has been used to date marine terraces and deposits but shells tend to act as open systems allowing additional uranium to be incorporated or the daughter products to be lost (Kaufman et al. 1971). Hence, shell dates are unreliable and may be in error by a large amount. Bone is also commonly dated by this method but is subject to the same problems when acting as an open system. Using both U-series to date the same specimen has proven useful as a test; a concordant age may indicate a closed system and therefore a valid date.

Ku et al. (1977) have used U-series analysis of pedogenic carbonate to directly date desert soils. Because carbonate is continually being added to the soil system, care must be taken to isolate the innermost and oldest carbonate precipitates in the Cca and K horizons of calcic soils.

Peat, speliothem carbonate, cave carbonate accretions and deep-sea sediments have also been dated by U-series techniques. For most substances, though, problematic results for some samples have cast doubt on its reliability with the possible exception of fossil coral (if the aragonite shells have not recrystallized).

Fission Track

This method is used with volcanic glass shards or crystals such as zircon which contain minute spontaneous fission tracks resulting from atomic decay and is generally useful for ashes older than about 10^5 years. Many crystals or shards are usually counted optically to ascertain an average value. The density of fission tracks increases with age, all other things being equal. Error for this method usually originates from one of two sources; human error in counting and track annealing. Counting may be in error when using glass shards because small tubules may resemble fission tracks. More commonly, annealing may result from a brief high-temperature event, a lengthy low-temperature history, or by a high-pressure event (Boellstorff and Steineck 1975). If loss of spontaneous tracks occurs, the age estimate will be too young.

Chemical Methods

Enantiomeric ratios (D/L) of fossil mollusk amino acids yield relative and absolute age estimates of Quaternary marine deposits from about 10^3 to 10^6 years B.P. (Wehmiller et al. 1978). Only L enantiomers exist in mollusks and almost all other living organisms while alive, but convert spontaneously to D enantiomers upon death. This racemization process is reversible and eventually, an equilibrium D/L ratio equal to one is ascertained.

The racemization process is highly temperature dependent and the effective diagenetic temperatures must be, but seldom are, known. This method, therefore, usually provides only relative ages which must be calibrated by other absolute methods, such as U-series dates on coral, for different areas and latitudes. Once calibrated, D/L ratios for shells on adjacent terraces will provide absolute ages. Local temperature anomalies and perturbations after burial provide one of the most significant sources of error and will probably remain the limiting factor for this technique.

Obsidian hydration and tephra superhydration are similar techniques dealing with the rate of chemical diagenesis in volcanic glass. Fresh glass is out of equilibrium because of its low water content and will hydrate to form perlite with time. The hydration changes the refractive index of the glass and causes a rind to form around the glass shard. In general, the thicker the rind, the older the tephra unit. Accuracy is generally about ± 10%. Once the glass is completely hydrated, small vesicles in the glass will fill with water resulting in superhydration. The latter process tends to be less precise than hydration but allows for approximate dating of late Pleistocene ashes. The hydration technique has proven useful in Holocene archeologic studies in accessing the age of obsidian projectile points.

Weathering and Soil Development

Many disciplines interrelate when applied to weathering phenomena. Studies on the rates of weathering rind development on clasts incorporated in glacial tills (Coleman and Pierce 1981) or other deposits, determination of seismic velocities in clasts as a function of age (Crook et al. 1978; Gillespie 1982), rates of saprolite development and rates of soil profile development are all related to weathering of a parent material as a function of age.

Relative soil profile development, because of its versatility and range, is becoming one of the most widely used tools for temporal control when radiometric age determinations at a site are not available. Soils continue to develop through time in nearly all parts of the world (providing the soil remains at the surface) making them useful in assessing very old deposits (10^6 years) as well as relatively young ones (10^1–10^4 years). There are, however, many variables which need to be clarified or assessed in order to arrive at reasonable age assignments, and it is necessary to regionally calibrate a soil-chronosequence (a set of soils arranged by age) using radiometric or other dating methods before the chronology is applied to sites where absolute dates are not available. With constraint, soil ages are generally good to ± 25% of the true age of the deposit (Birkeland 1974).

Soil formation (S) is a function (f) of principally five factors; parent material (p), topography or relief (r), climate (c), organic matter or biota (o), and time (t) and can be expressed as an equation:

$$S = f(p,r,c,o,t) \tag{2}$$

(Jenny 1941). More generally, Simonson (1959) expresses soil formation as a function (f) of the product of additions (a), removals (r), transformations (t_1) and translocations (t_2) of material from the profile:

$$S = f(a,r,t_1,t_2). \tag{3}$$

Runge (1973) emphasizes water as the organizing vector in pedogenesis and modifies Jenny's equation to:

$$S = f(w,o,t) \tag{4}$$

where w is the soil energy related to water throughflow, o is the organic matter or biotic influence and t is time. This model suggests that concentration of water flow through the soil profile results in stronger profile development at that site. More recently, Johnson and Rockwell (1982) and Johnson et al. (in progress) advance a supplementary model that strength of soil formation may be expressed as:

$$S = f\left(P, K, \frac{dP}{dt}, \frac{dK}{dt}\right) \tag{5}$$

where S is the strength of soil formation of an entire solum or a single attribute of the solum, P and K are the sets of passive and kinetic factors such as parent material, soil chemical environment, water table level, stability of the geomorphic surface, energy and mass fluxes, frequency of wetting and drying cycles, and pedoturbation. The dP/dt and dK/dt factors access the effect of how the passive and kinetic factors have changed with time such as increased Pleistocene precipitation, and the derivative of the expression (S) with respect to time (dS/dt) is the rate of soil development. The above models complement each other in that they allow workers to evaluate different aspects of soil formation and weathering phenomena.

In general, several basic properties of soils are useful as initial age indicators, since most or all increase with time. These are: depth to unweathered parent material, thickness of the B horizon, thickness of the B_{2t} horizon, color of the B horizon (under oxidizing conditions), thickness and abundance of clay films in the B_{2t} horizon (until destroyed by shrinking and swelling), texture, consistance and ped structure. These properties, all based on field morphological descriptions, have been quantified by various workers (Harden 1982; Bilzi and Ciolkosz 1977; Meixner and Singer 1981) and allow for a determination of relative age for soils of different terraces or surfaces within a region where parent material does not vary much. The rate of soil development for any particular area, however, must still be calibrated using absolute methods.

Quaternary Timescales

The timescale applied is dependent on the purpose of the investigation or research. If the goal is the siting of a critical facility such as a nuclear power plant, the timescale used may be a broad one encompassing much of the Quaternary. On the other hand, study of the response of a particular fluvial system to sea level rise near the coast or to changing climatic conditions may require a timescale of 10^4 to 10^5 years.

The Pleistocene is defined by fossil flora and fauna and is associated with late Cenozoic glaciation. Hence, the timescale used to define the Pleistocene should accordingly be of similar basis. Until recently, four major glacial events recognized from the mid-continent of the U.S. and Europe, were tentatively correlated and used as the basis for a general time scale. However, analysis of deep-sea sediment cores and $^{18}O/^{16}O$ ratios indicates many more than four periods of glaciation (Emiliani 1955, 1966; Shackleton and Opdyke 1973) (Fig. 1) calling for a revision of the classical timescale.

Recent work on the dating of uplifted fossil coral reefs in New Guinea and Barbados (Bloom et al. 1974; Bender et al. 1979; Broecker et al. 1968), as well as many other areas of the world has provided an excellent calibration for ice-volume curves derived from oxygen-isotope ratios, both temporally and spatially with respect to the level of the ocean during interglacial and glacial periods over the past 250,000 years and longer. Sea level fluctuations and hence periods of major glaciation follow ɔd as:

(5)

ı single attribute of
ɩuch as parent ma-
he geomorphic sur-
ycles, and pedotur-
passive and kinetic
ecipitation, and the
e rate of soil devel-
y allow workers to
ımena.
itial age indicators,
ıthered parent ma-
lor of the B horizon
lms in the B_{2t} hori-
ınce and ped struc-
iptions, have been
1977; Meixner and
ɔils of different ter-
ot vary much. The
t still be calibrated

igation or research.
ver plant, the time-
rnary. On the other
level rise near the
ɔf 10^4 to 10^5 years.
ıssociated with late
istocene should ac-
events recognized
ɔorrelated and used
sea sediment cores
ılaciation (Emiliani
vision of the classi-

w Guinea and Bar-
8), as well as many
r ice-volume curves
ılly with respect to
er the past 250,000
or glaciation follow

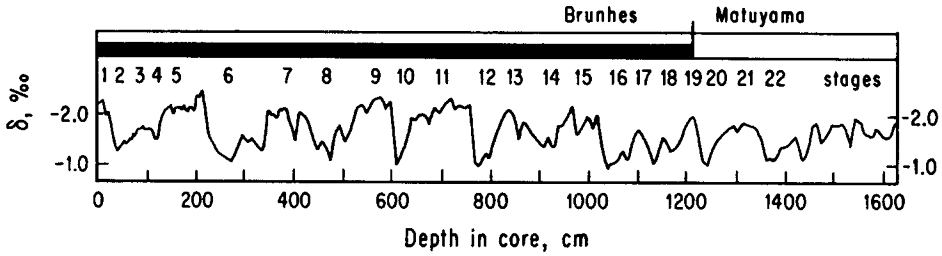

Fig. 1. Oxygen-isotope ($^{18}O/^{16}O$) ratios for deep-sea core V28-238 (after Shackleton and Opdyke 1973). Sea-level highstands and interglacial periods correspond to odd intergers and sea-level lowstands or glacial periods correspond to even intergers. The Brunhes-Matuyama magnetic boundary is at about 700×10^3 years. B.P.

a periodic trend which parallels cycles in tilt and procession of the earth's axis causing summer insolation (Broecker et al. 1968) and has a major frequency of approximately 100×10^3 years.

The timescale used for the correlation of high and low sea level stands was proposed by Emiliani (1955); periods of highstand (interstadials or interglacials) are assigned odd valued numbers and periods of sea level lowstand (glacial advance) are assigned even integers (Fig. 1). Presently, we are in Stage 1. Stage 2 corresponds to the late Wisconsin full glacial period, Stage 3 to the mid-Wisconsin interstadial, Stage 4 to early Wisconsin glaciation and Stage 5 to the last major interglacial. Similarly, major glacials and interglacials stepping back in time as viewed from the oxygen-isotope record, correspond to progressively larger numbers. Each major number or period may be subdivided based on minor fluctuations; Stage 5 is subdivided into 5a, 5b, 5c, 5d, and 5e with a, c, and e letters corresponding to high sea level stands and 5b and 5d to lower sea level periods. Use of this type of timescale may cover the entire Pleistocene but is most useful for the past few hundred thousand years for which terraces and deposits are dated and correlated worldwide. Additonally, correlation of the sea-level record to continental and alpine glacial events is fairly easy for "Illinoian" or Stage 6 and younger sediments but becomes increasingly more difficult back in time due to the lack of datable material and confident stratigraphic correlations.

There is direct applicability of sea-level and climatic fluctuations to dating deposits at or near the coast or in northern and alpine regions. The former areas were directly effected by eustatic sea-level lowering and rising; strath and fill terraces often are a direct result of such base level changes or climatic change. Similarly, marine terraces correlate directly to high sealevel stands and therefore provide an excellent indication of age for many abrasion platforms once one or two terraces in a region are dated. Mid-high latitude and alpine areas commonly contain Pleistocene glacial tills which may be either directly dated or correlated to known worldwide glacial advances. In tectonic geomorphology, it is important to recognize and distinguish deformed surfaces or deposits related to climatic perturbations in order to establish a chronology in lieu of or in conjunction with other more definite dating methods.

On a longer timescale, magnetic stratigraphy is very useful in determining relative and absolute ages of deposits. The base of the Pleistocene is generally drawn at the top of the Olduvai Normal Event (Bowen 1978) at about 1.8×10^6 years B.P. or at the base of the Olduvai Normal (Ericson and Wollin 1968) at about 2.0×10^6 years B.P. which roughly corresponds temporally with the onset of worldwide glaciation. Similarly, the base of the middle Pleistocene is drawn at the Brunhes-Matuyama boundary about 700×10^3 years B.P. and the base of the late Pleistocene at about 130×10^3 years B.P. at the beginning of the last interglacial (not a magnetic boundary) (Bowen 1978). All of these events are recognized worldwide facilitating correlation and dating.

The Pleistocene-Holocene boundary has been arbitrarily defined at about 10×10^3 to 11×10^3 years B.P. during a time of glacial retreat and eustatic sea-level rise. The boundary probably has important application in tectonic and engineering studies because faults which have moved during this time period are considered active.

The Quaternary timescale outlined above is summarized in Table 1, including the principal dating methods and their ranges of applicability. The boundaries may change in the future as more information accumulates but the general timescale will probably remain the same.

Geomorphic Indicators of Tectonic Activity and Paleoseismicity

Study of recent tectonic activity based upon geomorphic principles has taken two approaches depending upon whether reconnaissance information or more detailed information is needed or desired: 1. development of indices related to rock resistance and/or climatic change and/or tectonic activity useful in reconnaissance work; and 2. more detailed process-response models that attempt to analyze relations between landforms, geomorphic processes and earth materials integrated through time.

Geomorphic Indices

Geomorphic indices are useful reconnaissance tools in tectonic geomorphology because they generally may be obtained quickly from measurements taken from topographic maps, aerial photographs or field survey and provide insight concerning adjustment of bedrock and landforms to tectonic and/or climatic perturbations. Indices that have been successfully used are generally related to erosional and depositional processes associated with the fluvial system. The best known of these are the stream-gradient index (SL index) developed by Hack (1973), mountain front sinuosity (Bull and McFadden 1977) and the ratio of valley floor width to valley height (Bull and McFadden 1977).

The stream-gradient (SL) index developed by Hack (1973) and applied to the Transverse Ranges of southern California (Keller 1977) is defined for a particular stream reach, as:

$$SL = \frac{\Delta H}{\Delta L} L \qquad (6)$$

where: SL is the stream gradient index, $\Delta H/\Delta L$ is the stream gradient or channel gradient of the reach (ΔH is the change in elevation of the reach and ΔL is the reach length), and L is the channel length from the drainage divide at the longest stream in the basin to the center of the reach being evaluated (see Fig. 2).

The index is, according to Hack (1973), significant because it is crudely related to available stream power which reflects the ability of the stream to transport the load and the channel morphology that provides the resistance to flow. This results because the available stream power is proportional to the product of the discharge and water surface slope; upstream channel length is proportional to bankfull discharge, which is thought to be important in forming and maintaining stream channels, and the slope of the water surface over a particular reach may be approximated by the slope of the channel through that reach.

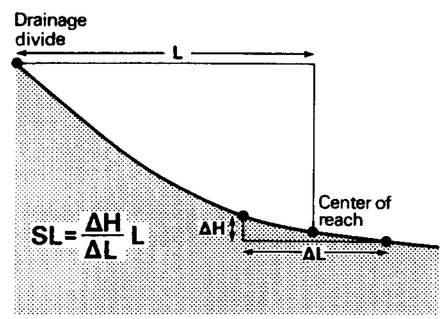

Fig. 2. Idealized diagram showing how the stream gradient (SL) index is calculated (after Hack 1973)

The stream-gradient index is particularly sensitive to changes in slope and thus is a valuable reconnaissance tool in evaluating relations between rock resistance, possible tectonic activity, and topography. That the index is sensitive to rock resistance is demonstrated by the long profile of the Potomac River from its junction with the South Branch to Washington D.C. (Fig. 3). Average stream-gradient indices along the profile vary from about 130 to 870 gradient m, and are relatively low where the river flows over softer sedimentary rocks in the upper part of the profile. Indices increase diametrically where the river flows over the relatively resistant rocks of the Blue Ridge, decrease across the softer rocks of the Triassic Basin, and increase again where the river again crosses resistant rocks at Great Falls (see Fig. 3). Thus in the Appalachian Mountains of the eastern United States there is a good relationship between rock resistance and values of the stream-gradient index. In tectonically active areas, we may capitalize on this by looking for areas with anomalously high stream-gradient indices for a particular rock resistance. It is assumed that streams may adjust quickly to both tectonic and climatic perturbations and therefore anomalously high indices should be related to either very resistant rocks or maladjustment of the fluvial system to tectonic activity and/or recent climatic change. Figure 4 shows stream-gradient indices for the San Gabriel Mountains in southern California. Areas of anomalously high indices occur along the southern and eastern fronts of the range and relatively low indices are found on the softer rocks, some of which are along the San Andreas and San Gabriel fault zones where strike-slip (horizontal) deformation has crushed the rocks. Although it was previously known that rates of

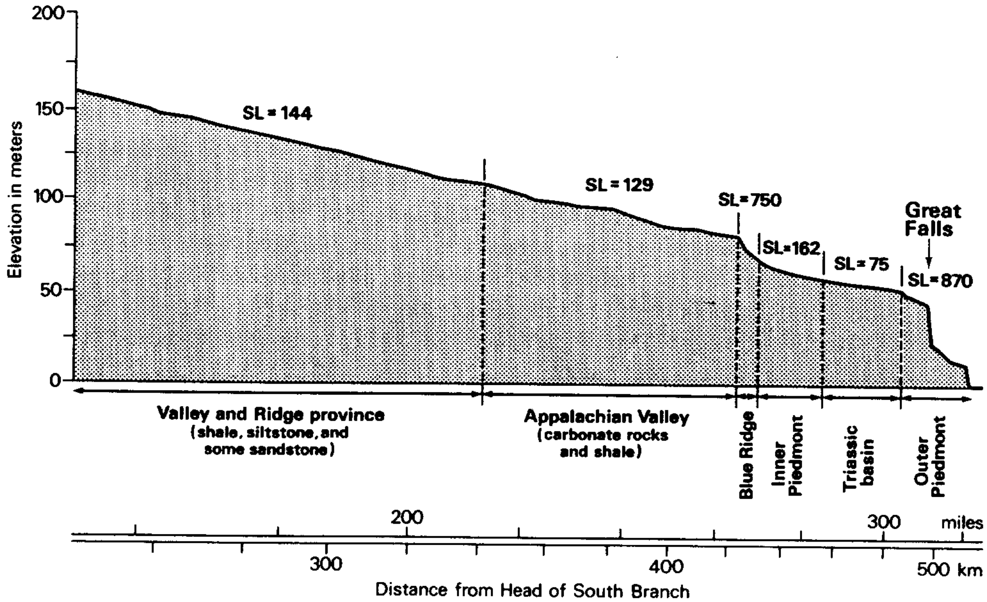

Fig. 3. Stream gradient (SL) indices along the Potomac River upstream from Washington D.C., see text for explanation. (after Hack 1973)

uplift are relatively high on several areas of the south and southeastern flanks of the San Gabriel Mountains, the indices tended to verify this and interestingly, there is an area of anomalously high indices near the location of the San Fernando earthquake of 1971. Thus, it appears that the stream gradient index is a potentially valuable tool when performing reconnaissance work using relatively small scale (1 : 50,000 to 1 : 250,000) topographic maps. The technique has the added advantage that analysis of elevation data stored in computer systems is possible. Thus, in theory, large areas may be evaluated quickly. Interpretation of the index, however, will remain crude because it is difficult to separate the effects of rock resistance from recent tectonics.

Two additional geomorphic indices are mountain-front sinuosity and the ratio of valley floor width to valley height (relief) (Bull and McFadden 1977). Mountain front sinuosity (S_{mf}) is defined as:

$$S_{mf} = \frac{L_{mf}}{L_s} \tag{7}$$

where L_{mf} is the length of the mountain front along the mountain-piedmont junction and L_s is the straight line length of the mountain front. The S_{mf} index, according to Bull and McFadden, reflects a balance between the tendency of uplift to maintain a relatively straight front and the work of streams that erode to produce a more irregular or sinuous front. Tectonically active areas characterized by relatively rapid uplift along faults bounding mountain ranges will have straight fronts compared to those ranges where tectonic activity has slowed down or ceased. Thus, as a mountain front retreats due to erosion from streams that cross the front following cessation or slowing of uplift, mountain-front sinuosity increases with time.

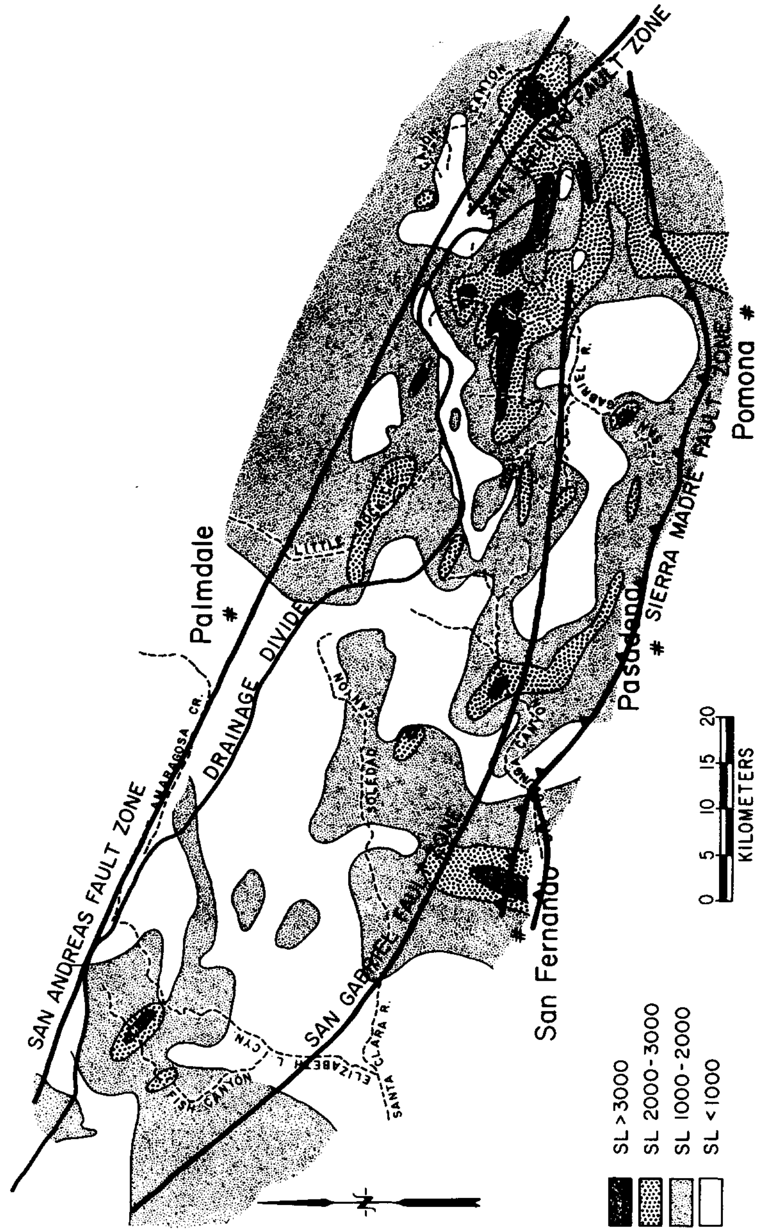

Fig. 4. Stream gradient (SL) indices, San Gabriel Mountains, southern California

The ratio of valley floor width to valley height (V_f) is an index defined as:

$$V_f = \frac{2\,V_{fw}}{(E_{ld} - E_{sc}) + (E_{rd} - E_{sc})} \tag{8}$$

where V_{fw} is the width of the valley floor, E_{ld} and E_{rd}, respectively are the elevations of the left and right valley divides, and E_{sc} is the elevation of the valley floor or stream channel (Bull and McFadden 1977). The V_f index reflects differences between "V" shaped canyons and broad-floored canyons emerging from mountain fronts. The data is taken from a given distance upstream from a mountain front; comparison of valleys emerging from different mountain fronts or different parts of the same front provides an index that indicates whether the stream is actively downcutting in response to range front tectonic activity or where it is eroding laterally into adjacent hillslopes due to relative base level stability (Bull and McFadden 1977).

Geomorphic indices, mountain-front sinuosity and the ratio of valley floor width to valley height, were applied by Bull and McFadden (1977) to evaluate the tectonic geomorphology north and south of the Garlock fault in southern California. The indices, along with alluvial fan morphology, were used to classify mountain fronts into three groups: 1. active tectonism characterized by relatively low mountain-front sinuosity (S_{mf}) and low values of the ratio of valley floor width to valley height (V_f); 2. moderate to slightly active tectonism, characterized by intermediate values of S_{mf} and V_f; and 3. slightly to no active tectonism characterized by high S_{mf} and V_f values. Bull and McFadden's study suggests that there is marked contrast in tectonic activity north and south of the Garlock fault. North of the fault, low values of the S_{mf} and V_f indices suggest that mountain fronts are tectonically active, whereas south of the fault, the same indices suggest tectonic stability. Thus these indices, as with the stream-gradient index, are valuable in reconnaissance of an area or region by delineating areas where further study is warranted.

Process-Response Models in Tectonic Geomorphology

Process-response models, broadly defined to include study of landforms and Quaternary stratigraphy, are more site specific in tectonic geomorphology studies than the use of geomorphic indices, and imply the coupling of specific geomorphic processes with a response involving the production of deposits and/or landforms. For example, processes of erosion and deposition may produce an alluvial sequence of stream, marsh, lake, or landslide deposits that may be subsequently or concurrently faulted. Study of these deposits may illuminate the magnitude and frequency of past earthquakes (see for example Clark et al. 1972; Sieh 1978; Davis 1981; Rust 1982). Faulting may also produce discrete or compound fault scarps, the morphology of which may be studied to help understand the paleoseismicity of an area or region (Wallace 1977). Finally, study of specific landforms such as alluvial fans (Bull 1964, 1977; Hooke 1972; Keller et al. 1982a; Rockwell and Keller 1980), marine terraces (Matsuda et al. 1978; Lajoie et al. 1979), fluvial terraces (Lensen 1968; Keller et al. 1982b) as well as assemblages of landforms such as sag ponds, pressure ridges, horsts and garbens, shutter ridges, deflected drainage, and offset drainages (Dibblee 1977; Sieh 1978; Trifonov 1978; Schubert 1982; Keller et al. 1982a) are useful as geomorphic indicators of recent tectonic activity and paleoseismicity.

Faulted Holocene Deposits

Processes of erosion and deposition produce alluvial sequences of marsh, stream, or lake deposits, as well as landslide and debris flow deposits. Such deposits of late Pleistocene to Holocene age when faulted, provide valuable information concerning the paleoseismicity of a fault. To illustrate this, we will discuss two examples from the San Andreas fault system in southern California.

Holocene activity and paleoseismicity on the Coyote Creek fault (part of the San Jacinto fault zone which is a major branch of the San Andreas fault system in the Salton Basin of southern California) was determined by studying progressive vertical displacement of Holocene lake deposits (Clark et al. 1972; Sharp 1981). Recurrence interval (RI) in years for an earthquake of given magnitude and displacement may be defined as:

$$RI = \frac{Dpe}{Sr} \tag{9}$$

where Dpe is the estimated displacement per event and Sr is the slip rate for the fault.

The April 9, 1968 Borrego Mountain Earthquake ($M_s = 6.7$) on the Coyote Creek fault produced, along with predominant right lateral displacement, localized vertical displacement. Although the vertical displacement at 12 field sites varied from 0 to 100 mm, the most representative value is estimated to be 70–100 mm (Clark et al. 1972). Detailed work across a fault scarp presumably produced by several past events of faulting suggests that a lake deposit dated at 435 ± 75 dendrochronologically corrected ^{14}C years B.P. has been displaced by approximately 450 mm of vertical fault slip. Thus the vertical slip rate at this site is 450 mm/435 years, or about 1.0 mm/year. If it is assumed that the 450 mm of vertical fault slip resulted from a series of events similar to the 1968 event and that each past event also had 70 to 100 mm of vertical displacement then the recurrence interval for this type of moderate event (M_s 6.7) is, from (9), 70 to 100 years. Sharp (1981) has constrained the horizontal slip rate for this fault to between 3 and 5 mm/year over the last 435 years using the same fault data and new age control of the sediments. At another site, Sharp (1981) documents 10.9 m horizontal displacement of a stream channel incised into mid-Holocene lake beds. The age of detrital charcoal within the fluvial deposits indicates an age of about 5200 dendrochronologically corrected ^{14}C years B.P. and yields a longer term slip rate of about 2 mm/year, significantly lower than the late Holocene or historic rate. Sharp (1967, 1981) also has determined 6.6 to 8.6 km of right slip for a fluvial and lacustrine deposit dated by tephrachronologic correlation at 0.73×10^6 years B.P. This yields a long term mid to late Pleistocene slip rate of 8 to 12 mm/year, considerably higher than the Holocene or even late Holocene rate. These data indicate that the Coyote Creek fault is active, has had recurrence of moderate magnitude earthquakes ($M_s \sim 6.5$) throughout the Holocene with a recurrence interval ranging from perhaps as low as every 50 years to several hundred years, depending on the time frame discussed. Of significance to the present earthquake hazard is the apparent reduction of the late Holocene and historic rate of faulting.

A common question concerning the San Andreas fault north of Los Angeles, California is: How often do large earthquakes occur? Data from 55 km northeast of Los Angeles at Pallett Creek (Sieh 1978) and at two other sites up to 125 km northwest of Pallett Creek (Davis 1981; Rust 1982) suggest that three large events since the 16th century may be correlated. At Pallett Creek, (a small intermittent stream that crosses the San Andreas fault near the base of the San Gabriel Mountains) Sieh (1978) believes there is evidence for twelve large earthquakes in the last 1700 years, (one historic, in 1857, and eleven prehistoric) providing an average recurrence of about 145 years. However, the length of time between any two earthquakes may vary from as short as 50 years to as long as 300 years (Sieh 1978).

The remarkable record of paleoseismicity at Pallett Creek is a result of an unusual set of fortuitous conditions. First there is a nearly continuous 2000 year record of late Holocene sedimentation consisting of fluvial gravel, sand, and silt. Interspersed peat and units containing charcoal, wood and other organic materials suitable for ^{14}C dating provide precise temporal control. Second, the deposits have been repeatedly faulted by movement along the San Andreas fault; and third, modern incision has lowered the water table and exposed the faulted section (Sieh 1978). Thus, tectonic processes that have produced the San Gabriel Mountains have also provided the energy to erode sediments and deposit them in and adjacent to Pallett Creek. Therefore, to read the history of the uplift of mountains and the earthquakes along associated faults, one must examine the sediments deposited and faulted at the foot of the mountains. The trick is to find the right place where the process-response situation has produced an intact and preserved record such as at Pallett Creek, which evidently is not very common.

Alluvial Fans

Alluvial fans are the end points of erosional-depositional systems in which sediment eroded from mountain source areas is transported to mountain front areas where it is intermittently deposited as a cone of fan-shaped body of fluvial and/or debris-flow deposits (Bull 1977). Bull (1977) states, "The stream is the connecting link between the erosional and depositional parts of the system, and is a dominant influence on the fan morphology. Changes in stream-channel slope, depth and width affect the slope, loci and mode of deposition. Such changes may be caused by changes in discharge of sediment and water, mode of transport or by tectonic events." As these changes occur, fan slope adjusts producing the observed radial profile composed of a series of straight segments which together are gently concave. Breaks in slope mark boundaries of the segments, and younger segments can be recognized from older segments by examining soil profile development or relative weathering of clasts (see Bull 1964 and 1977 for a more detailed discussion of segmented alluvial fans).

Alluvial fan morphology is an indicator of recent tectonic activity because it reflects varying rates of tectonic processes (uplift of the mountain) relative to fluvial processes in both the mountain (erosional) and alluvian fan (depositional) parts of the system. Relations between various parts and processes may be summarized (Bull 1977) by examining rates of uplift of the mountain front ($\Delta u/\Delta t$); stream channel downcutting in the mountain ($\Delta w/\Delta t$); and fan deposition ($\Delta d/\Delta t$) or erosion ($\Delta e/\Delta t$). When

$$\frac{\Delta u}{\Delta t} \geqq \frac{\Delta w}{\Delta t} + \frac{\Delta d}{\Delta t} \qquad (10)$$

then, assuming some de
uplift exceeds downcutt
Thus, with active uplift,
stream emerges from th
upstream into the mour
uplift (see Fig. 5A). Thi
alluvial fan deposits are
uplift of the mountain is
in the mountain and fan
alluvial fan deposits (Bu
On the other hand, v

$$\frac{\Delta u}{\Delta t} < \frac{\Delta w}{\Delta t} > \frac{\Delta e}{\Delta t}$$

then the rate of uplift c
stream and fan depositi
entrenched. Thus, the y
of the fan (Bull 1964, 19
Fan head trenching
the rate of uplift exceed
entrenchment is only te
relation (10) (Bull 1964,
Bull's model has be
south end of Death Va
ferential normal faultin
small and steep on the
lation 10 applies), and
as in Fig. 5A. On the o
not as steep, and not a
and the youngest fan se

Fault Scarp Morpholog

Scarps produced direct
duced by erosion along
phic processes of erosi
the term "degraded fau
not always easy, but the
degraded fault scarp. F
fault-line scarp and it
from the fault that for
cerned with young fault
relief to fault displacer
these, recognizing that
Slopes are dynami
slope elements, each o
slope elements associat

then, assuming some deposition on the fan occurs (that is $\Delta d/\Delta t > 0$), the rate of uplift exceeds downcutting and deposition occurs adjacent to the mountain front. Thus, with active uplift, the youngest deposits (fan segments) are located where the stream emerges from the mountains, and in many cases the fan deposits will extend upstream into the mountain valley as the stream attempts to adjust its slope to the uplift (see Fig. 5 A). This relationship (10, above) explains why thick sequences of alluvial fan deposits are often associated with orogenic periods; as long as the rate of uplift of the mountain is greater than or equal to the sum of the rates of downcutting in the mountain and fan deposition, then conditions favor the accumulation of thick alluvial fan deposits (Bull 1964, 1977).

On the other hand, when

$$\frac{\Delta u}{\Delta t} < \frac{\Delta w}{\Delta t} > \frac{\Delta e}{\Delta t} \tag{11}$$

then the rate of uplift of the mountain is less than the rate of downcutting of the stream and fan deposition is shifted down-fan (see Fig. 5 B) as the fanhead becomes entrenched. Thus, the youngest fan deposits (or fan segments) are located at the toe of the fan (Bull 1964, 1977).

Fan head trenching can also occur in response to climatic variations even though the rate of uplift exceeds the rate of downcutting ($\Delta u/\Delta t > \Delta w/\Delta t$). However such entrenchment is only temporary and backfilling would be expected as predicted by relation (10) (Bull 1964, 1977).

Bull's model has been successfully tested (Hooke 1972) for alluvial fans at the south end of Death Valley, California. Hooke found that eastward tilting and differential normal faulting produced segmented alluvial fans. The fans are relatively small and steep on the east side of the valley where active downfaulting occurs (relation 10 applies), and the youngest fan segments are generally near the fan-heads as in Fig. 5 A. On the other hand, fans on the west side of Death Valley are larger, not as steep, and not as influenced by mountain front uplift (relation 11 applies), and the youngest fan segments are near the toes of fans, analogous to Fig. 5 B.

Fault Scarp Morphology

Scarps produced directly by faulting are called "fault scarps", whereas those produced by erosion along a fault are "fault-line scarps". Where near-surface geomorphic processes of erosion and deposition have significantly modified a fault scarp, the term "degraded fault scarp" is appropriate. Differentiating between the three is not always easy, but there is an evolution in form and process from a fault scarp to a degraded fault scarp. Furthermore, a scarp on the down-thrown block of a fault is a fault-line scarp and it might also be argued that a scarp that has retreated away from the fault that formed it is also a fault-line scarp. Our discussion here is concerned with young fault scarps and degraded fault scarps that still owe their original relief to fault displacement. We shall use the term fault scarp to refer to both of these, recognizing that most are degraded to varying degrees.

Slopes are dynamicy changing landforms composed of distinct (but related) slope elements, each of which forms a slope segment. Figure 6 shows generalized slope elements associated with a fault scarp. All of the elements may not be present

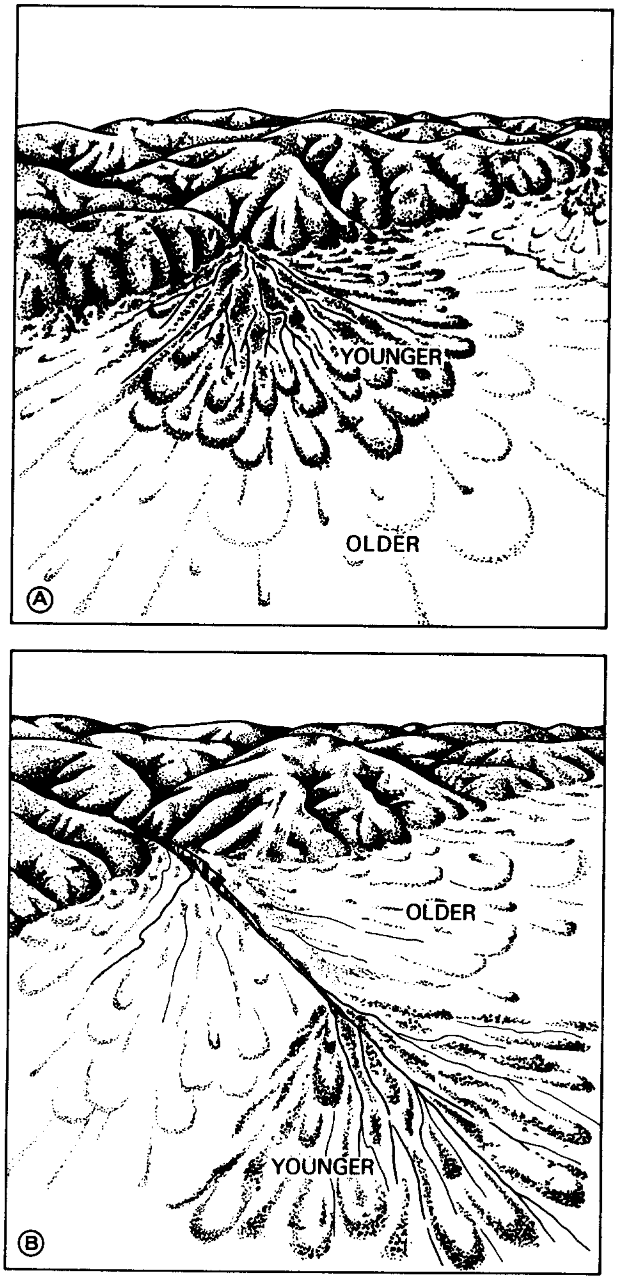

Fig. 5. Alluvial fan morphology. Deposition adjacent to mountain front (A), and deposition shifted down-fan resulting in fanhead entrenchment (B). (After Bull 1977)

Fig. 6. Generalized slop
ments relevant to a fault
(after Wallace 1977)

Fig. 7. Change in fault s
gy-process with time,
Basin area in Nevada.
explanation (after Walla

on a particular fault
changes with time. T
scarp morphology a
Nevada.

Assuming that th
active in the late Qu
the earthquake risk
(shown on Fig. 7) b
scarps that truncate
Lahontan, scarps ass
with trees that may b

Recurrent displac
that multiple displac
on the fault scarp pr

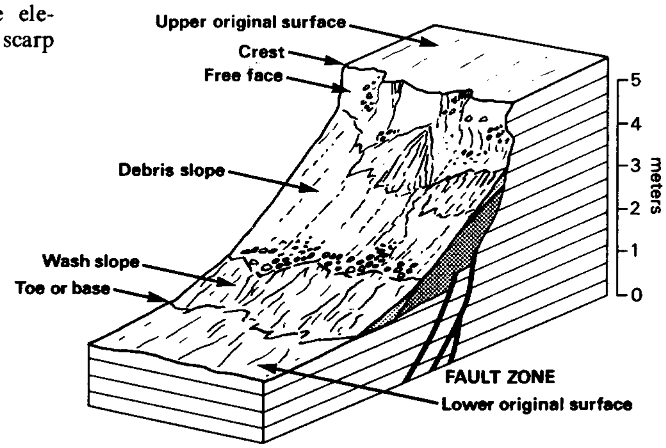

Fig. 6. Generalized slope elements relevant to a fault scarp (after Wallace 1977)

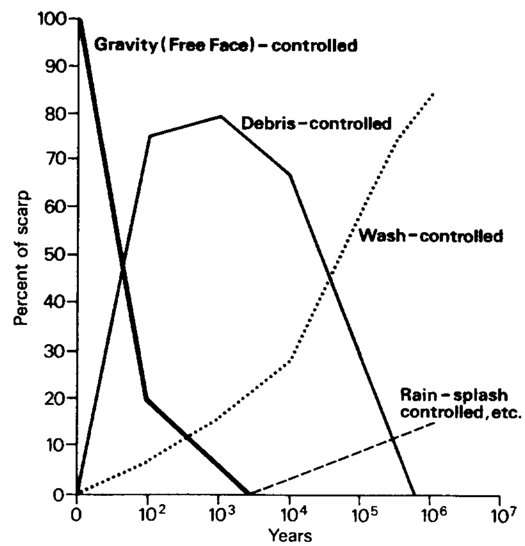

Fig. 7. Change in fault scarp morphology-process with time, for the Great Basin area in Nevada. See Table 3 for explanation (after Wallace 1977)

on a particular fault scarp, and the dominance of one element relative to others changes with time. Table 3 and Fig. 7 summarize form-process relations for fault scarp morphology as presented by Wallace (1977) for the Great Basin area in Nevada.

Assuming that the scarps result from seismic events (earthquakes) along faults active in the late Quaternary, then study of their morphology is one way to assess the earthquake risk or hazard. Wallace (1977) was able to develop a chronology (shown on Fig. 7) by studying fault scarps produced from known earthquakes, scarps that truncate or are truncated by ^{14}C dated shorelines of Pleistocene Lake Lahontan, scarps associated with volcanic ash of known age, and scarps associated with trees that may be dated by counting tree rings (dendrochronology).

Recurrent displacement produces a composite fault scarp. Wallace (1977) states that multiple displacements may be recognized by: 1. pronounced breaks in slope on the fault scarp profile; 2. benches or terraces located along channels that have

Table 3. Fault scarp-slope morphology (after Wallace 1977, for fault scarps in the Great Basin, USA)

Slope element	Morphology	Process (formation and/or modification)	Comments and general chronology
Crest	Top of fault scarp (break in slope); initially sharp, becomes rounded with time	Produced by faulting; modified by weathering, mass wasting	Becomes rounded after free face disappears; usually rounded after about 10,000 years
Free face	Straight segment; initially 45° to overhanging	Produced by faulting; modified by weathering, gullying, mass wasting; eventually buried from below by accumulation of debris	Dominant element for 100 years or so; disappears after about 1,000–2,000 years
Debris slope	Straight segment; at angle of repose of material usually 30 to 38°	Accumulation of material that has fallen down from the free face	Is dominant element after about 100 years, remains dominant until about 100,000 years; disappears at about 1,000,000 years
Wash slope	Straight to gently concave segment; overlaps the debris slope; slope angle generally 3 to 15°	Fluvial erosion and deposition; deposition of wedge or fan of alluvium near toe of the slope; some gullying	Is developed by 100 years; significant by 1,000 years; and dominant by 100,000 years
Toe	Base of fault scarp (break in slope) slope; may be initially sharp, but with time may become indeterminate as grades into original slope	Fluvial erosion and deposition; owes to change in process/form from upslope element (free face, debris slope, or wash slope) to original surface below the fault scarp slope	More prominent in young fault scarps or where wash slope is not present. On scarps older than about 12,000 years the basal slope break is sharper than the crestal slope break

eroded through the scarp; 3. knickpoints along channels that cut across the scarp; 4. scarp height (toe to crest) that exceeds the maximum recorded height for a single event; and 5. progressive displacement (older materials are displaced more than younger).

A quantitative treatment of the geomorphology of fault scarps is provided by Bucknam and Anderson (1979), who developed relations between scarp-height and scarp-slope-angle for fault scarps in western Utah with estimated ages ranging from 10^3 and 10^5 years B.P. (Fig. 8). These authors verified and further quantified Wallace's (1977) contention that for scarps of a given height, older scarps will be degraded to a lower slope-angle. Thus, for example in Fig. 8, the scarp-slope-angle for a scarp with constant height of 3 m decreases from about 28° to 10° as the age of the scarp increases from about 10^3 to 10^5 years B.P. These curves may then be applied to other scarps in the region of known heights to estimate the late Quaternary earthquake hazard and history.

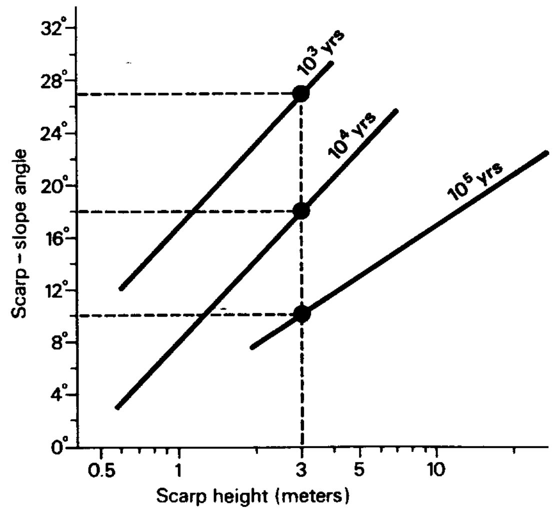

Fig. 8. Relation between fault scarp, slope angle and scarp height for western Utah. (after Bucknam and Anderson 1979)

Terraces

Marine and fluvial terraces are significant surfaces (landforms) in tectonic geomorphology because they are reference points from which to study rates of tilting, folding, uplift, and faulting.

Correlation of terraces over a large area or region based on relative position and elevation in active tectonic areas may not be possible because a particular terrace may be found at various elevations. For example a marine terrace near Ventura, California, dated by both U-series and amino acid racemization at 40,000 to 60,000 years B.P., varies in elevation from below sea level near Carpenteria, California to about 350 m only 11 km to the southeast towards Ventura (Lajoie et al. 1982). Similarly, a terrace of the Ventura River dated at about 38,000 ^{14}C B.P. varies in elevation from 40 m to at least 80 m above the river (Keller et al. 1982b; Rockwell et al., in press). Deformation of both terraces is due to tilting, folding and faulting associated with regional and local deformation producing the western Transverse Ranges of southern California.

Significant tectonic information may be gained from studying a flight (or series) of late Pleistocene and Holocene terraces (with known absolute ages) deformed by local faulting and folding and/or regional uplift. Questions that may be asked are: 1. have rates of deformation been constant through time; 2. which faults have been most active in the Holocene; 3. how do slip rates on faults vary in time and space; 4. are historic rates of deformation (based upon first-order surveying) verified in the recent geologic record; and 5. what is the likely displacement per event and recurrence interval (RI) of earthquakes on seismically active faults? Answers to these questions along with other geologic information will obviously be very important in evaluating the seismic risk associated with a particular fault or group of faults in an area.

Marine terraces are erosional, wave cut surfaces, platforms or benches that slope gently away from the shore and are covered with a thin veneer of marine sands beneath a variable amount of terrestrial sediment deposited by fluvial, eolian and/or

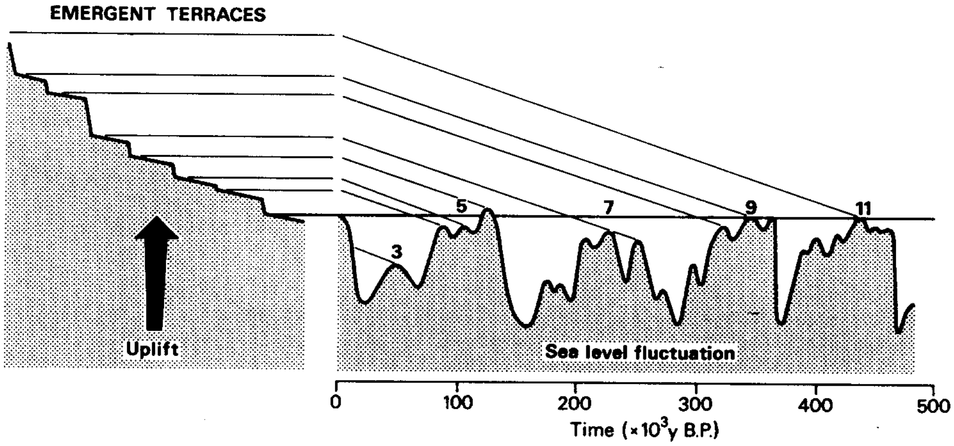

Fig. 9. Idealized diagram showing how emergent marine terraces, associated with tectonic uplift and Pleistocene sea level changes, are produced. (after Lajoie et al. 1979)

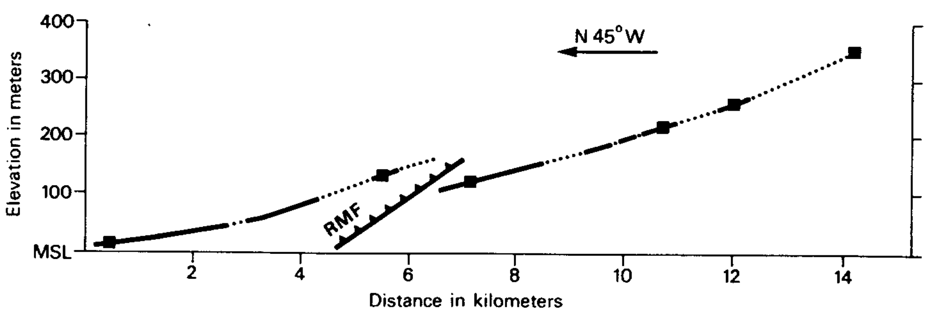

Fig. 10. Profile of the Carpenteria-Punta Gorda marine terrace (age, 40,000–60,000 years B.P.). Uplift to the southeast is due to folding. Notice north-side-up displacement across the Red Mountain fault (RMF). (after Lajoie et al. 1982)

mass wasting processes. Figure 9 illustrates how a series of emergent marine terraces might form in response to uplift. It is significant to recognize that the age of the bedrock erosion surface may be quite different (older) from the age of the terrestrial cover sediments, thus care must be taken when evaluating terrace chronology. From a tectonic geomorphology view, the most important part of a marine terrace is the shoreline angle, defined as the line of intersection of the wave-cut platform with the seacliff (Lajoie et al. 1979). The shoreline angle is significant because it is a reference from which to measure tectonic deformation. That is, in tectonically active areas, profiles of terrace remnants, constructed from elevations taken as close as possible to the shoreline angle, should identify locations where the originally horizontal shoreline angle has been deformed by faulting or folding. Figure 10 shows the profile of the Carpenteria-Punta Gorda terrace (age 40,000–60,000 years B.P.). Notice the deformation across the Red Mountain fault and increase in elevation to the southeast as the terrace is deformed by uplift associated with the active Ventura Avenue anticline (Lajoie et al. 1982).

Study of marin
potential seismic ri
marine terraces 50
sult from sudden u
angle, right-lateral
along the Sagami
Sea plate and the
uplift is from est
(M ≧ 8) that occu
those seismic even
Holocene terraces

Fig. 11. Uplift ass
and 1923 (**B**) eartl
Japan (after Mats
interval in m

Study of marine terraces can also help evaluate the recurrence interval (RI) and potential seismic risk of an area. Matsuda et al. (1978) studied a series of emergent marine terraces 50–100 km south of Tokyo, Japan. The emergence is believed to result from sudden uplift of several meters during large earthquakes produced by low-angle, right-lateral faulting with a thrust component. The active tectonic zone is along the Sagami trough, part of the convergent boundary between the Philippine Sea plate and the Asian plate (see Fig. 11). Evidence for the hypothesis of sudden uplift is from estimated and measured uplift during two historic earthquakes ($M \geqq 8$) that occurred in 1703 and 1923. Figure 11 shows the uplift associated with those seismic events, and Fig. 12 shows the altitude and chronologic position of four Holocene terraces at the southern end of the Boso Peninsula. These data suggest

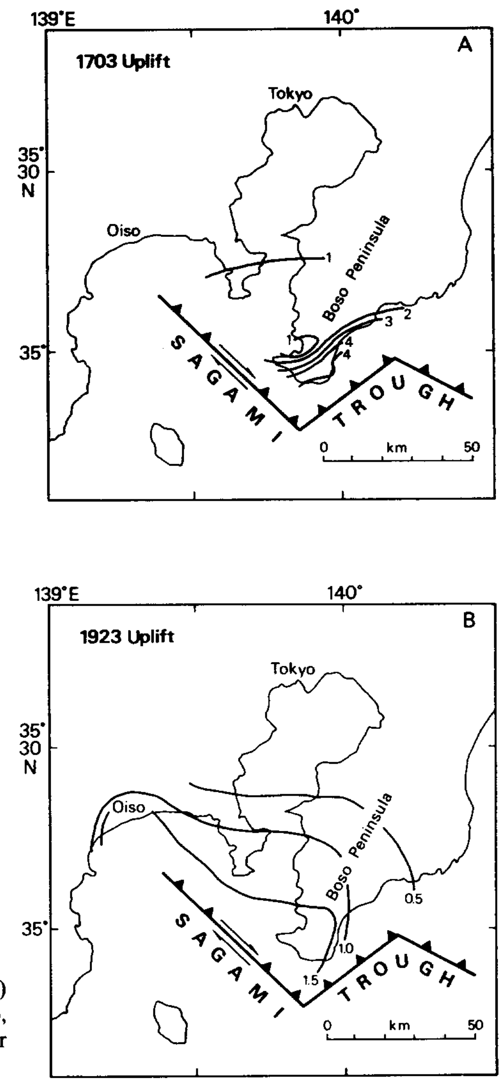

Fig. 11. Uplift associated with the 1703 (**A**) and 1923 (**B**) earthquakes south of Tokyo, Japan (after Matsuda et al. 1978). Contour interval in m

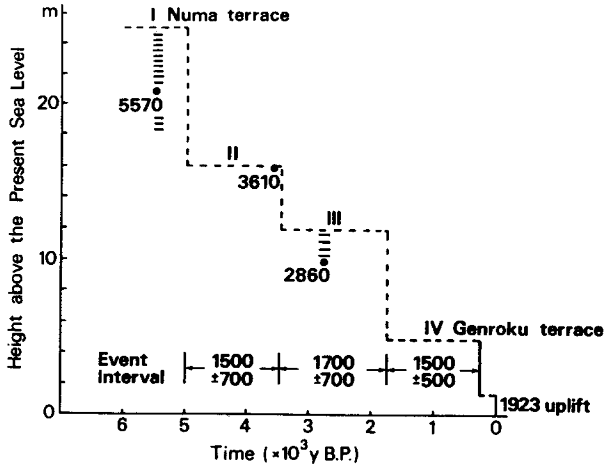

Fig. 12. Altitude and chronology of four Holocene marine terraces at the southern end of the Boso Peninsula, Japan. (after Matsuda et al. 1978)

that there have been four large earthquakes in the last 6,000 years, and event intervals (see Fig. 12) suggest that the recurrence interval for these earthquakes is approximately 1,500 years. Matsuda et al. (1978) also concluded that the Oiso area (see Fig. 11) is a likely candidate for a large earthquake in the relatively near future. They believe this because the uplift of the Oiso area during the 1703 earthquake was negligible, even through Holocene activity, as recorded by the position of the 6,000 years old Numa terrace, suggests that prior to the 1703 event (during the period between 6,000 and 2000–3,000 years B.P.) the Oiso area had experienced uplift comparable to the southern Boso Peninsula, that is about 20 m, presumably produced by 4 or 5 large earthquakes. However, at present the Numa terrace, as a result of the 1703 earthquake, is a few meters higher at the Boso Peninsula than near Oiso. Thus the rate of uplift during the last 2,000–3,000 years for the Oiso area is less than the regional average during the last 6,000 years and may be in a recent seismic gap that could be filled by a large earthquake in the relatively near future.

Fluvial terraces are also a useful reference point for studying rates of tectonic activity and the potential earthquake hazard. For example, Lensen and Vella (1971) studied a flight of seven terraces along the Waiohine River, New Zealand, that were progressively offset during the late Pleistocene and Holocene by the Wairarapa fault. The dominant active displacement as suggested by the offset terraces is right-lateral with a vertical component. The fault produced a major earthquake, accompanied by an unknown amount of horizontal and vertical displacement in 1855. The terraces were formed as the river cut down through the Waiohine surface (an alluvial fan) during the late Pleistocene and Holocene. Development of a terrace chronology, lacking absolute dates, was accomplished by assuming an age for the Waiohine surface, based on glacial stratigraphy, of 20,000 to 35,000 years B.P. This estimated age of the fan, with a measured horizontal offset of 120 m for the fan surface, provides a horizontal slip rate of 3.4 to 6.0 mm/year. Assuming a constant slip rate and applying it to known horizontal displacements allowed assigning estimated ages to the terraces. Lenson and Vella (1971) also assumed a 3 m horizontal dis-

Terraces

placement per event
ducing comparable (
A similar study
placed by left-latera
et al. (1981). A date
measured horizontal
ly provides a late Pl
respectively. Althou
the Nobi fault syste
placement, produce
ments during that e
that the Atera fault
quake is 8 m, and de
fault. However, such
geomorphologically
ance that the seismi
concerning the hist
short to determine t
the late Pleistocene
estimate paleoseism
further discussion of
nese scientists in the
it appears that in th
earthquakes. Evide
represent collapse
speculation that the
(Sieh 1981). Thus, it
large earthquakes o
(1,600 years) from t
A study of sever
fornia, progressively
has provided impo
rupture hazard in t
1981), as well as sli
nology was develop
placement on faults
Most faults shown
fault, are flexural-sl
in response to foldi
where large earthq
significant regional
Some of the bes
race surfaces towar
fined. The cross-sec
face.
The most promi
by two independent

placement per event to estimate a RI of 500 to 900 years for large earthquakes producing comparable (3 m) displacements.

A similar study of a flight of nine terraces of the Kiso River, progressively displaced by left-lateral slip along the Atera fault in Japan, is discussed in Yoshikawa et al. (1981). A date of about 27,000 ^{14}C years B.P. on one of the older terraces with measured horizontal and vertical displacement of about 140 m and 28 m respectively provides a late Pleistocene average slip rate of about 5 mm/year and 1 mm/year respectively. Although the Atera fault has no certain record of historic movement, the Nobi fault system 60 km to the east, with similar orientation and sense of displacement, produced a M = 8.4 earthquake in 1891. The largest strike-slip displacements during that event were 8 m (Yoshikawa et al. 1981). It is tempting to assume that the Atera fault behaves similarly, that is slip per event from a M = 8.4 earthquake is 8 m, and derive a RI of about 1,600 years for this type of event on the Atera fault. However, such an assumption is risky because even though the faults appear geomorphologically similar and are in the same tectonic setting, there is no assurance that the seismic behavior is also similar. This brings up an important principle concerning the historic behavior of earthquakes; the historic record is often too short to determine the earthquake hazard of a particular fault. Thus we must look to the late Pleistocene and Holocene geologic record, as was done at Pallett Creek, to estimate paleoseismicity and future, potential seismic risk (See Allen 1975, for a further discussion of this principle). This approach has recently been taken by Japanese scientists in their study of the Atera fault, and although the record is complex, it appears that in the last 13,000 years there probably have been at least four large earthquakes. Evidence for individual events is from dated deposits assumed to represent collapse of fault scarps shortly after earthquakes. There is also some speculation that the Atera fault produced a historical large earthquake in 762 A.D. (Sieh 1981). Thus, it appears that a recurrence interval of several thousand years for large earthquakes on the Atera fault is reasonable, and similar to that derived above (1,600 years) from the sequence of offset river terraces.

A study of several late Pleistocene terraces to the Ventura River near Ojai, California, progressively displaced by several active and potentially active reverse faults, has provided important information concerning the seismic shaking and ground rupture hazard in the area (Clark and Keller 1979, 1980; Clark 1980; Yeats et al. 1981), as well as slip rates for individual faults (Rockwell et al., in press). The chronology was developed utilizing ^{14}C dates, relative soil profile development, and displacement on faults. The most prominent terraces and faults are shown on Fig. 13. Most faults shown on Fig. 13 with the exception of the Santa Ana-Arroyo Parida fault, are flexural-slip induced and displacement is parallel to bedding. Faulting is in response to folding of the bedrock, and displacement does not extend to depths where large earthquakes are produced. Thus flexural-slip faults do not produce a significant regional seismic shaking hazard.

Some of the best evidence for the flexural slip hypothesis is the tilting of the terrace surfaces toward the axis of the Ayers Creek syncline to which the faults are confined. The cross-section on Fig. 13 shows tilting of the 55,000 year old (Qt6b) surface.

The most prominent terrace (Qt6a) is about 38,000 ^{14}C years B.P., as established by two independent ^{14}C dates. Ages of surfaces younger than Qt6a were established

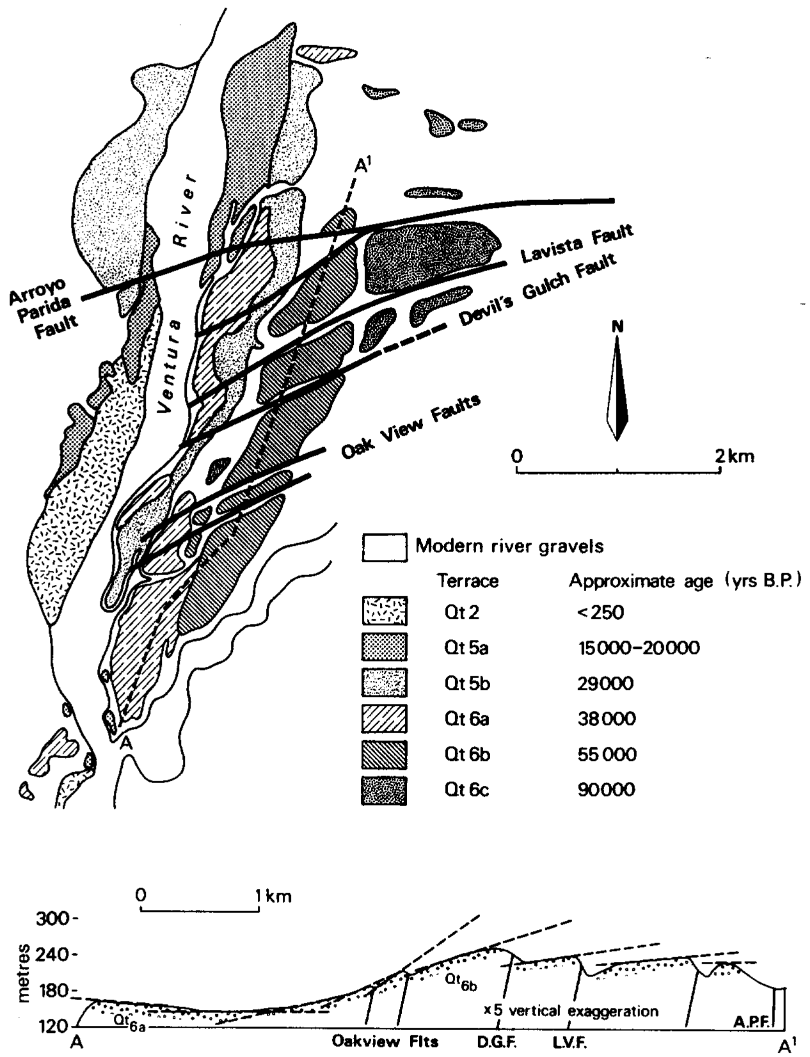

Fig. 13. Fluvial terraces of the Venture River, California, deformed by folding and faulting. (after Keller et al. 1982b)

from ^{14}C dates and correlation by soil profile development. For older surfaces (Qt6b and Qt6c), terrace chronology was established by using the vertical slip rate of the Arroyo Parida fault (0.4 mm/year), which was shown to be constant during the latest Pleistocene (Rockwell et al., in press), with known vertical displacement of older terrace surfaces displaced by the Arroyo Parida fault. Therefore, given a constant slip rate, the age of a surface is approximately the amount of vertical displacement divided by the slip rate. The chronology was then applied to known vertical displacements on flexural-slip faults to calculate slip rates varying from 0.3 to 1.1 mm per year. Because fault scarps are often several tens of meters high and have

Holocene displacement
There are very little da
one event near Lompo
about 25 cm of vertical
1981). Assuming that th
then recurrence interval

Stream terraces have
For examples, terraces o
fornia are being folde
1942; Keller et al. 198
profiling correlated, dat
used to derive rates of t
ing at crests of anticlin
areas of active folding i
nition indicates areas w

Landform Assemblage a

A genetic classification
cesses tend to produce a
of landforms. Strike-sli
ed streams, offset and
micro-topography (sma
14 shows some of these

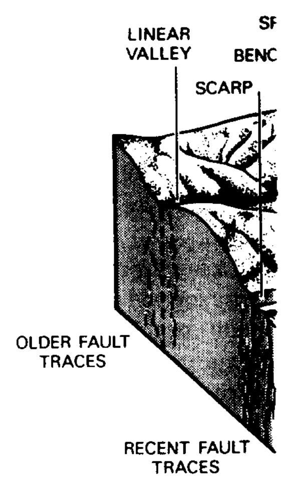

Holocene displacement, the faults do present potential ground rupture hazard. There are very little data concerning historic displacement on flexural-slip faults; one event near Lompoc, California, in 1981 produced a M=2.5 earthquake and about 25 cm of vertical displacement along a 570 m surface rupture (Yerkes et al. 1981). Assuming that the flexural-slip faults near Ojai can produce similar events, then recurrence intervals would vary from 250 to 750 years.

Stream terraces have also been valuable landforms in the study of recent folding. For examples, terraces of the Shinano River in Japan and the Ventura River in California are being folded by active tectonism (Yoshikawa et al. 1981; Putnam 1942; Keller et al. 1982b). Folding of late Pleistocene terraces is best studied by profiling correlated, dated terrace segments over fold axes. The profiles can then be used to derive rates of tilting on the limbs of folds and rates of uplift or downwarping at crests of anticlines or troughs of synclines respectively. Simply identifying areas of active folding is significant in tectonic geomorphology because such recognition indicates areas where active faulting may also be expected.

Landform Assemblage and Strike-Slip Faulting

A genetic classification of landforms is possible because specific geomorphic processes tend to produce a particular set of responses that produce a given assemblage of landforms. Strike-slip faulting, for example, produces landforms such as beheaded streams, offset and/or deflected streams, sags, shutter ridges, pressure ridges, micro-topography (small horsts and grabens), linear valleys and fault scarps. Figure 14 shows some of these in diagrammatic form, and Fig. 15 shows several fault relat-

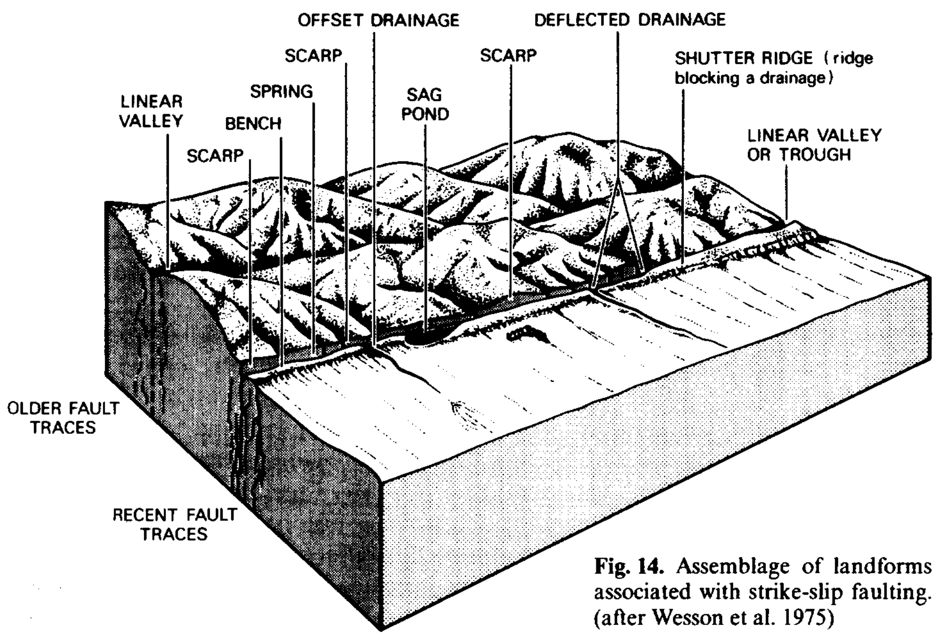

Fig. 14. Assemblage of landforms associated with strike-slip faulting. (after Wesson et al. 1975)

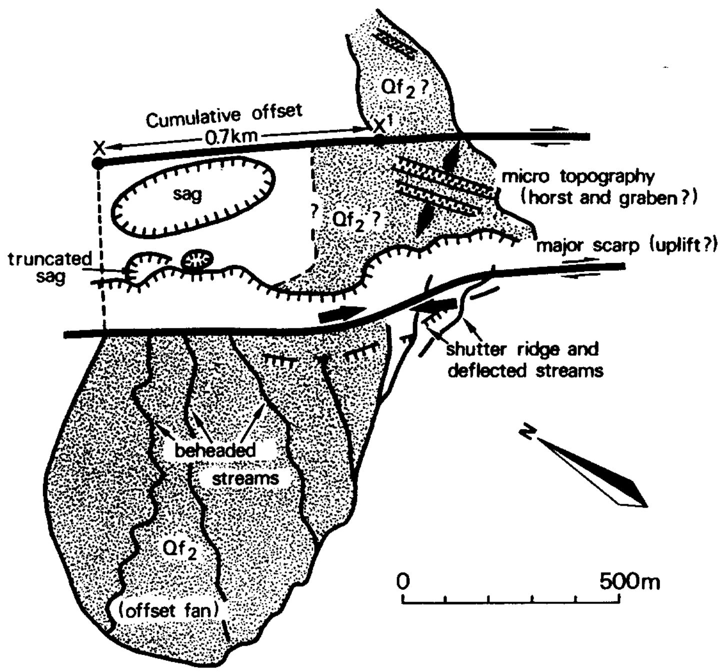

Fig. 15. Fault-related landforms associated with an alluvial fan offset along the San Andreas fault near Indio, California

ed landforms associated with an offset alluvial fan located along the San Andreas fault at the base of the Indio Hills, east of Palm Springs, California.

Some of the landforms associated with strike-slip faulting, as well as the orientation of fractures, folds, and normal and reverse faults, can be explained by extension and contraction associated with simple shear in a strike-slip tectonic framework (Keller et al. 1982a) (Fig. 16). Other landforms associated with strike-slip tectonics, such as sags (small pull-apart basins) or pressure ridges (small uplifts or squeeze ups) can be explained by steps or sharp bends in the main trace of the fault as shown in Fig. 17 (Crowell 1974; Dibblee 1977). On a larger scale, Crowell (1974) and Dibblee (1977) suggest that some of the major late Cenozoic basins and uplifts in southern California have developed in response to more complex strike-slip tectonics associated with large steps or gentle bends of the San Andreas fault. In this context, a basin such as the Salton Trough can be thought of as a large pull-apart. Other basins such as Ridge Basin, north of Los Angeles, apparently formed by weak crustal rocks sagging as they moved around a gentle releasing (right) bend along the San Andreas fault. On the other hand, uplift, which is producing the Indio Hills northwest of Palm Springs and the San Gabriel Mountains north of Los Angeles, may be associated with gentle restraining (left) bends of the San Andreas fault. An important ingredient in understanding the tectonic history is determining which fault traces were active at particular times, as this influences the chronology of deformation associated with strike-slip faulting. A general conclusion emerges: in very active tectonic areas the geomorphology (topography) is an important indicator of

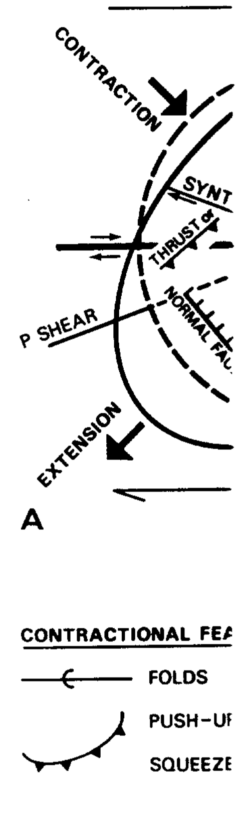

Fig. 16. Orientation
slip fault zone (A afte
sociated with strike-s
strike-slip fault such
left lateral system are

the recent deforma
uplifted, and there
pographic position
to be transitory fro
Study of landf
paleoseismicity of
particularly impor
measurable amour
can be obtained. L
the offset feature h
accurately; and 2.

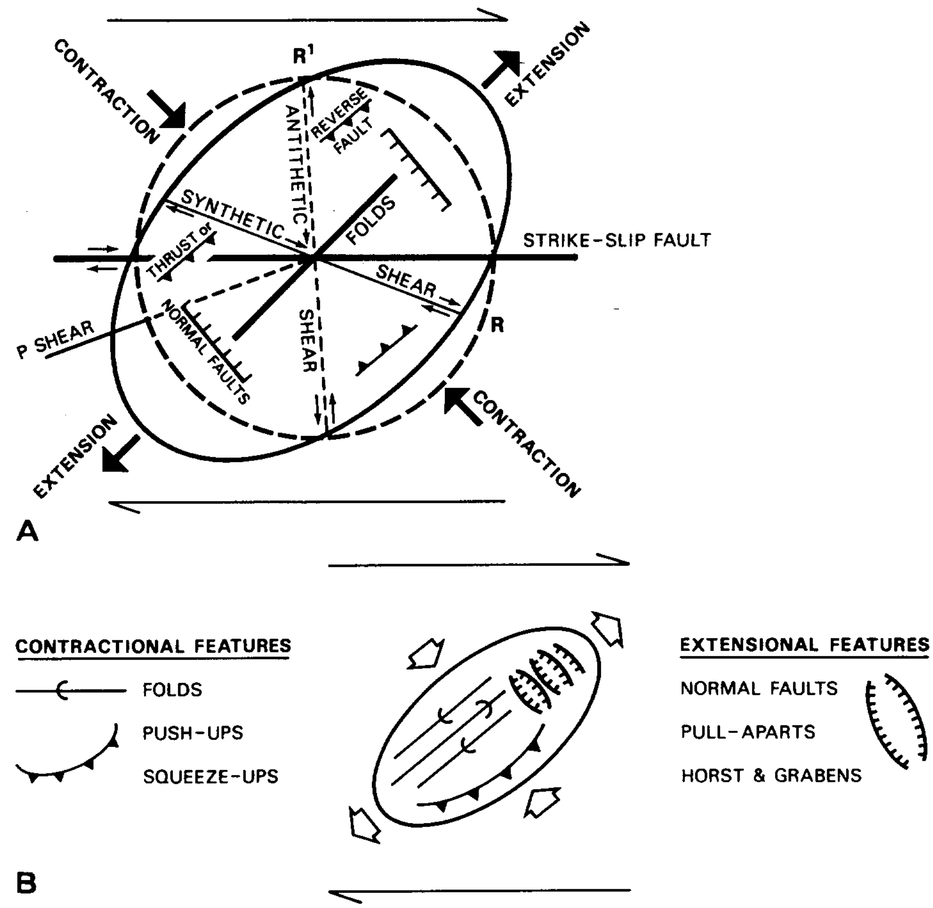

Fig. 16. Orientation of shear fractures, faults and folds associated with simple shear in a strike-slip fault zone (**A** after Sylvester and Smith 1976). Extensional and contractional landforms associated with strike-slip faulting (**B** after Keller et al. 1982a). **A** and **B** are for a right lateral strike-slip fault such as the San Andreas fault. Orientations of fractures, folds and faults in a left lateral system are in response to a strain elipse rotated 90° to that shown

the recent deformation. That is, topographic highs are areas that have been recently uplifted, and there may be localized disequilibrium between rock resistance and topographic position (eg., weak rocks on ridges). However, such disequilibrium tends to be transitory from a geologic perspective.

Study of landforms associated with strike-slip faulting can help evaluate the paleoseismicity of a particular fault or section of a fault. Features that have been particularly important are glacial and fluvial landforms/deposits which are offset a measurable amount and for which a reliable date (necessary to calculate a slip rate) can be obtained. Late Pleistocene and Holocene slip rates are most reliable when 1. the offset feature has clear boundaries so that the amount of offset can be measured accurately; and 2. a reliable absolute date for the feature can be obtained. Un-

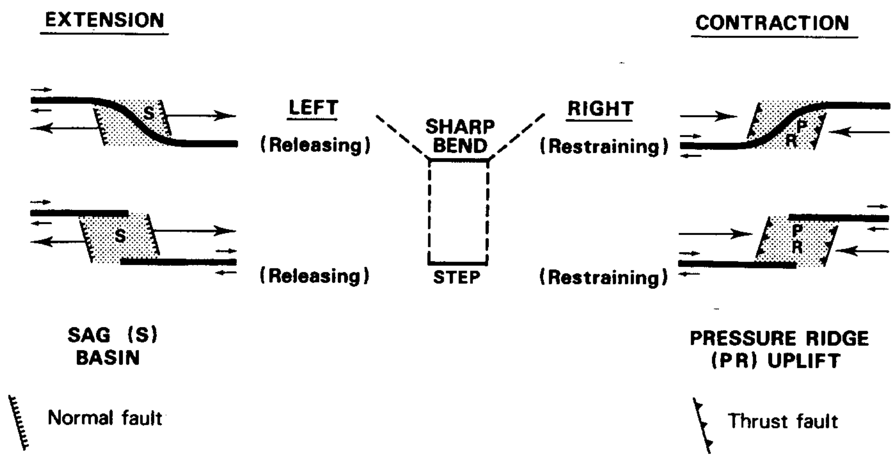

Fig. 17. Idealized diagram showing localized uplift and subsidence associated with bends and steps of right lateral, strike-slip fault traces. See text for further explanation. (after Crowell 1974; Dibblee 1977)

fortunately there are few cases where both of these criteria can be met. Thus, we usually have a good measurement with an estimated date, good dates with estimated offset, or a location where both the offset and age are estimated. In general, it is easier to locate offset features than to establish chronology. Because of the uncertainties, slip rates are usually given as a range that reflects the magnitude of the uncertainties. For example, Sieh (1981) estimates from an offset stream channel of Wallace Creek along the south-central part of the San Andreas fault, that the slip rate during the late Holocene is between a minimum of 33 mm/year (130 m offset in no more than 3,900 ^{14}C years B.P.) and a maximum of 64 mm/year (380 mm offset in no less than 5,900 ^{14}C years B.P.). As shown by Fig. 18 the offset is appreciable,

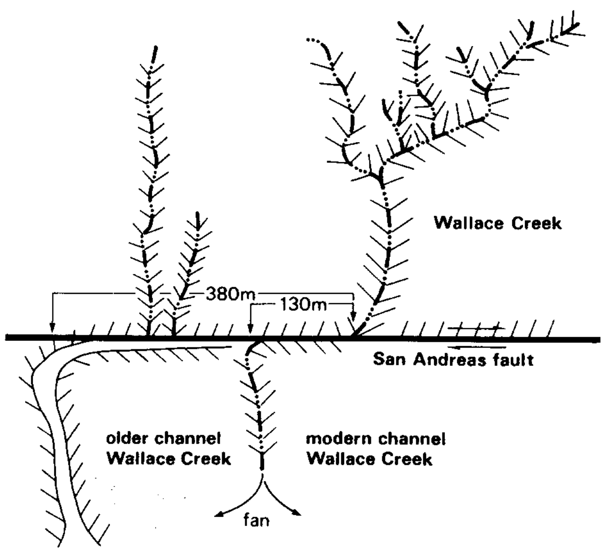

Fig. 18. Two offset channels of Wallace Creek along the San Andreas fault, California. (after Sieh 1981)

but ^{14}C dates, and the alluvial history of Wallace Creek, only provide approximate chronology of when the offsets occurred.

Further along the San Andreas fault, Keller et al. (1982a) evaluated an offset alluvial fan (Fig. 15). The cumulative offset of 700 m is farily good but the age of the fan deposits had to be estimated from soil profile development. The strongest statement that could be made was that the age of the fan may be as old as 70,000 years, but most likely is 20,000 to 30,000 years. Thus the slip rate since the late Pleistocene is estimated to be 10 to 35 mm/year, with a best estimate about 23 to 35 mm/year. As a final example, Schubert (1982) reports an estimated right-lateral slip rate for the Bocono fault in western Venezuela of 3 to 14 mm/year. This estimate is based on several measured offsets (60 to 250 m) of lateral moraines with an estimated age of 18,000 years, based on palynological, sedimentological and radiocarbon evidence.

The above three examples demonstrate some of the problems in obtaining slip rates for strike slip faults. Similar problems arise with normal and reverse faults. In spite of these shortcomings, study of active faults is providing important information from which slip rates and recurrence intervals for earthquakes can be calculated or estimated.

Neotectonics and the Earthquake Hazard

Historic Geodetic and Seismic Data

The historic record of earthquakes in the United States is very short geologically. Indeed, the record is very sketchy much beyond 200 years. Similarly, the historic record of geodetic measurements is even shorter. Allen (1975) has shown that for areas such as China or the Middle East where there is a 2,000–3,000 year record of earthquakes, major events in these regions show surprisingly large long-term temporal and spatial variations. Thus, it is not surprising that many moderate to large magnitude earthquakes have occurred in the United States on faults that were either unrecognized or which were not considered all that active. The 1971 San Fernando earthquake (M=6.6) in southern California is such an example: most of the individual fault strands were known to exist but were shown only on unpublished maps associated with tunnel construction by the local water district (Proctor et al. 1972). The individual strands that broke in 1971 were not recognized as being part of a major fault zone likely to produce such an earthquake.

Similar to historic fault ruptures, geodetic data provides only a small time window or reference frame for determining crustal movements. Nevertheless, determination of horizontal and vertical crustal movements has yielded invaluable data regarding actively deforming regions (Whitten 1956, 1960, 1971), stress accumulation across faults or regions (Thatcher 1976; Rodgers 1975; Savage et al. 1979; Savage and Burford 1970) and actual aseismic slip at depth (Savage et al. 1979) or at the surface in the form of fault creep (Bufe and Tocher 1974; Crough and Burford 1977; Nason and Weertman 1973). Leveling surveys also indicate which areas are going up or down regardless of the mechanisms or stresses involved. For instance, large areas which were previously covered by glaciers during the Pleistocene have been and are still recovering from the ice loading by isostatic rebound. This results in large areas of rapid uplift, yet only low to moderate seismicity. Alternatively, geodetic studies in areas undergoing active crustal folding and faulting indicate seismically active or potentially active regions (Buchanan-Banks et al. 1975).

Low-Shake Versus High-Shake Faults and Earthquake Hazard

It is a generally held belief that active faults produce damaging earthquakes. Recent work in southern California has indicated that there are types of active faults which are not likely to produce significant earthquakes (Yeats et al. 1981) and that these faults should be treated differently, once recognized. In the Ventura Basin in the Transverse Ranges Province of California, three general types of faults are recognized (see Fig. 19): those that produce ground rupture and seismic shaking (i.e., San Cayetano, Red Mountain, Santa Susana, and Arroyo Parida faults); those that produce seismic shaking but may not project to the surface to produce a ground rupture hazard (Oak Ridge fault); and those faults which produce ground rupture but little or no seismic shaking (Oak View faults, Orcutt and Timber Canyon faults). The first two categories are well documented in the literature in numerous localities but faults of the third type are not as well known.

"Low-shake" faults, those of the third category, may be formed by various mechanisms such as bedding plane slip within a syncline or out of the syncline fault-

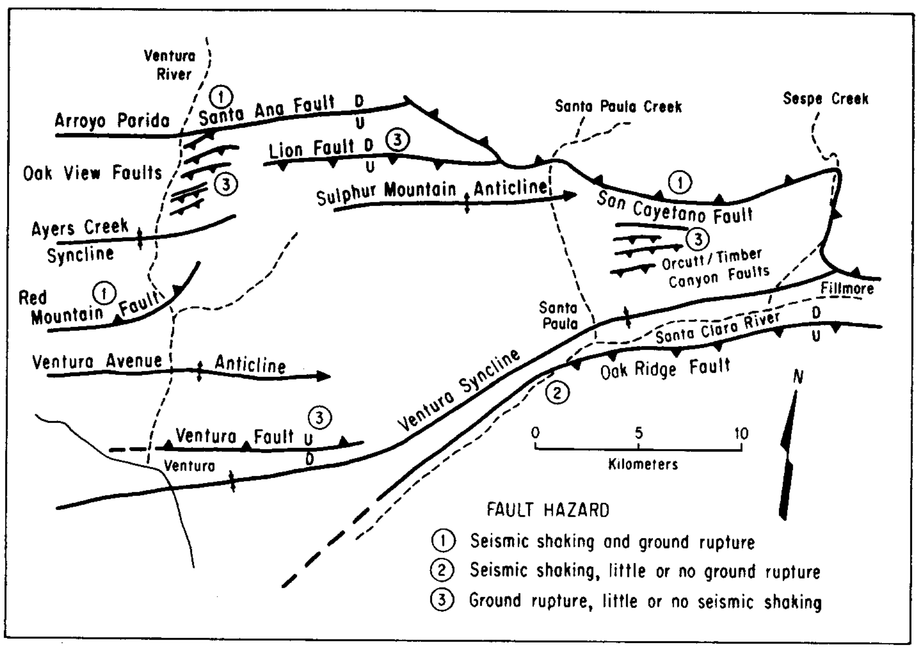

Fig. 19. Generalized geologic map of the central Ventura Basin, California, showing the earthquake hazard associated with individual faults

ing. They may cut sections at the surface or project up along bedding planes; the principal factor involved is their behavior at depth. Nearly all of these faults are due to folding and do not extend down into rocks of high shear strength. Accordingly, they are incapable of producing large magnitude earthquakes, although they may have high slip rates and display a large amount of late Pleistocene and Holocene ground rupture (Keller et al. 1980, 1982b; Rockwell and Keller 1980; Rockwell 1982; Clark and Keller 1980; Yeats 1982; Yeats et al. 1981).

Another type of low-shake faulting has been recognized as well: aseismic or micro-seismic slip along faults which are active due to groundwater or oil withdrawal. One such fault, the Buena Vista thrust in California, has been studied considerably (Koch 1933; Wilt 1958; Nason et al. 1968). This fault has documented slip rates varying between 11 and 33 mm/year between 1933 and 1967 (Nason et al. 1968). Surface features such as buckled oil pipelines and faulted paved roads were observed as well as subsurface well-case shearing. Similarly, normal faulting due to ground water withdrawal in the Antelope Valley, California has been documented with level lines and surface mapping; a slip rate of 35 mm/year for one of these faults is now well-documented (Sylvester 1982).

It is not known whether most of the movement along low-shake faults associated with folding is due to induced slip during nearby major earthquakes (regional deformation) or as a result of local deformation independent of more regional activities. Regardless, this type of faulting is being recognized in increasingly more places and earthquake hazard studies should not confuse this type of fault with those capable of producing large-magnitude events. Thus, the cause and nature of faulting is also important in seismic studies and it is regional as well as local studies which usually shed light on this aspect of tectonic activity.

References

Allen CR (1975) Geological criteria for evaluating seismicity. Geol Soc Am Bull 82:1041–1057

Bender ML, Fairbanks RG, Taylor FW, Matthews RK, Goddard JG, Broecker WS (1979) Uranium-series dating of the Pleistocene reef tracts of Barbados, West Indies. Geol Soc Am Bull Part 1, 90:577–594

Bilzi AF, Ciolkosz EJ (1977) A field morphology rating scale for evaluating pedological development. Soil Science 124 (1):45–48

Birkeland PW (1974) Pedology, weathering, and geomorphological research. Oxford Univ Press, New York, 285 p

Bloom AL, Broecker WS, Chappell JMA, Matthews RK, Mesolella KJ (1974) Quaternary sea level fluctuations on a tectonic coast. New $^{230}Th/^{238}U$ dates from the Huon Peninsula, New Guinea. Quat Res 4:185–205

Boellstorff DJ, Steineck PL (1975) The stratigraphic significance of fission track ages on volcanic ashes in the marine late-Cenozoic of southern California. Earth Planet Sci Lett 27:143–154

Bowen DQ (1978) Quaternary geology. Pergamon Press, New York, 221 p

Broecker WS, Thurber DL, Goddard J, Ku TL, Matthews RK, Mesolella KJ (1968) Milankovitch hypothesis supported by precise dating of coral reefs and deep-sea sediments. Science 159:297–300

Buchanan-Banks JF, Castle RO, Ziony JI (1975) Elevation changes in the central Transverse Ranges near Ventura, California. Tectonophysics 29:113–125

Bucknam RC, Anderson RE (1979) Estimation of fault-scarp ages from a scarp-height-slope-angle relationship. Geology 7: 11–14

Bufe CG, Tocher D (1974) Central San Andreas fault strain episodes, fault creep and earthquakes. Geology 2 (4): 205–207

Bull WB (1964) Geomorphology of segmented alluvial fans in western Fresno County, California. US Geol Surv Prof Pap 352-E: 89–129

Bull WB (1977) The alluvial fan environment. Prog Phys Geogr 1 (2): 222–270

Bull WB, McFadden LD (1977) Tectonic geomorphology north and south of the Garlock fault, California. In: Doehring DO (ed) Geomorphology in arid regions. Publ Geomorphol. Proc 8th Annu Geomorphol Symp. State Univ NY, Binghamton, pp 118–138

Chappel J (1974) Geology of coral terraces, Huon Peninsula, New Guinea: A study of Quaternary tectonic movements and sea-level changes. Geol Soc Am Bull 85: 553–570

Clark MC, Gantz A, Rubin M (1972) Holocene activity of the Coyote Creek fault as recorded in sediments of Lake Cahuilla. US Geol Surv Prof Pap 787: 112–130

Clark MN (1980) Ground rupture and seismic shaking as separate hazards of active faults. Proc 18th Annu Eng Geol Soils Eng Symp, Boise, Idaho, pp 83–96

Clark MN, Keller EA (1979) Newly identified zone of potentially active reverse faulting, western Transverse Ranges, California. Geol Soc. Am Abstr Programs 11 (7): 402–403

Clark MN, Keller EA (1980) Earthquake hazard evaluation of active faults near Ojai, California. Geol Soc Am Abstr Programs 12 (3): 102

Coleman SM, Pierce KL (1977) Summary table of Quaternary dating methods. Misc Field Stud US Geol Surv Map MF-904

Coleman SM, Pierce KL (1981) Weathering rinds on andesitic and basaltic stones as a Quaternary age indicator, western United States. US Geol Surv Prof Pap 1210: 56

Crook RJr, Allen CR, Kamb B, Payne CM, Proctor RJ (1978) Quaternary geology and seismic hazard of the Sierra Madre and associated faults, western San Gabriel Mountains, California. Final Tech Rep US Geol Surv Contract 14-08-0001-15258

Crough ST, Burford RO (1977) Empirical law for fault-creep events. Tectonophysics 42: T53–T59

Crowell JC (1974) Origin of late Cenozoic basins in southern California. In: Dickinson W (ed) Tectonics and sedimentation, Spec. Publ No 22. Soc Econ Paleontol Mineral, pp 190–204

Davis T (1981) Late Holocene seismic record, western Big Bend of San Andreas fault. Geol Soc Am Abstr Programs 13 (2): 51

Dibblee TW Jr (1977) Strike-slip tectonics of the San Andreas fault and its role in Cenozoic basic evolvement. In: Late Mesozoic and Cenozoic sedimentation and tectonics in California. San Joaquin Geol Soc Short Course, pp 26–38

Emiliani C (1955) Pleistocene temperatures. J Geol 63: 538–578

Emiliani C (1966) Paleotemperature analysis of Caribbean cores, P6304-8 and P6304-9 and a generalized temperature curve for the past 425,000 years. J Geol 74 (2): 109–126

Ericson DB, Wollin G (1968) Pleistocene climate and chronology in deep-sea sediments. Science 162: 1277–1284

Gillespie AR (1982) Quaternary glaciation and tectonism in the southeastern Sierra Nevada, Inyo County, California. Unpubl PhD thesis, California Inst Technol, 695 p

Gregory KJ (1978) A physical geography equation. Natl Geogr 12: 137–141

Hack JT (1973) Stream-profile analysis and stream gradient index. J Res US Geol Surv 1 (4): 421–429

Harden JW (1982) A quantitative index of soil development from field descriptions: Examples from a chronosequence in central California. Geoderma 28: 1–28

Hooke RL (1972) Geomorphic evidence for late-Wisconsin and Holocene tectonic deformation, Death Valley, California. Geol Soc Am Bull 83: 2073–2098

Jenny H (1941) Factors of soil formation. McGraw-Hill, New York, 281 p

Johnson DL, Rockwell TK (1982) Soil geomorphology: Theory, concepts and principles with examples and applications on alluvial and marine terraces in coastal California. Geol Soc Am Abstr Programs 14 (4): 176

Johnson DL, Keller EA, Rockwell TK, Dembroff GR (in prep) Differential dynamic-rate model of pedogenesis. Manuscript in preparation

Kaufman A, Broecker WS, Ku TL, Thurber DL (1971) The status of U-series methods of mollusk dating. Geochem Cosmochem Acta 35: 1155–1183

Keller EA (1977) A
work. Geol Soc
Keller EA, Bonkov
San Andreas fa
Am Bull 93: 46-
Keller EA, Rockw
phology of the
fornia. In: Coc
Meet Cordiller
Keller EA, Johnso
quake hazard,
81-376, 167 p
Klein J, Lerman J
carbon 24 (2):
Koch TW (1933)
Hills oil field,
Ku TL, Bull WB,
desert soils. Ge
Lajoie KR, Kern
RF, McCrory
to Santa Barb
California are
Lajoie KR, Sarna-
deformation ir
California. Gu
Lensen GJ (1968)
River terraces,
Lensen GJ, Vella
ments. R Soc
Mangerud J, Gull
way, Spitsberg
Matsuda T, Ota
major earthqu
Geol Soc Am
Meixner RE, Sing
tion and disco
Nason RE, Weert
Res 78 (32): 77
Nason RE, Coop
and oilfields,
pp 100–101
Olsson IU (1974)
Stockholm Fo
Olsson IU, Osad
^{14}C dating. B
Packer D, Bigga
Consultant R
Polach HA, Gols
of results. Au
Proctor RJ, Croo
ruptures, 19
83: 1601–161
Putnam WC (19
53: 691–754
Rockwell TK (1
western Tran
Rockwell TK, K
ern Transvers

Keller EA (1977) Adjustment of drainage to bedrock in regions of contrasting tectonic framework. Geol Soc Am Abstr Programs 9 (7): 1046

Keller EA, Bonkowski MS, Korsch RJ, Shlemon RJ (1982a) Tectonic geomorphology of the San Andreas fault zone in the southern Indio Hills, Coachella Valley, California. Geol Soc Am Bull 93:46–56

Keller EA, Rockwell TK, Clark MN, Dembroff GR, Johnson DL (1982b) Tectonic geomorphology of the Ventura, Ojai and Santa Paula areas, western Transverse Ranges, California. In: Cooper ID (ed) Neotectonics in southern California. Guideb Prep 78th Annu Meet Cordilleran Sect Geol Soc Am pp 25–42

Keller EA, Johnson DL, Clark MN, Rockwell TK (1980) Tectonic geomorphology and earthquake hazard, north flank, central Ventura Basin, California. US Geol Surv Open File Rep 81–376, 167 p

Klein J, Lerman JC, Damon PE, Ralph EK (1982) Calibration of radiocarbon dates. Radiocarbon 24 (2): pp 103–150

Koch TW (1933) Analysis and effects of current movement on an active fault in Buena Vista Hills oil field, Kern County, California. Am Assoc Petroleum Geol Bull 17 (8):694–712

Ku TL, Bull WB, Freeman ST, Knaus KG (1977) Th^{230}/U^{234} dating of pedogenic carbonates in desert soils. Geol Soc Am Abstr Programs 9 (7): 1061

Lajoie KR, Kern JP, Wehmiller JF, Kennedy GL, Mathieson SA, Sarna-Wojcicki AM, Yerkes RF, McCrory PF (1979) Quaternary marine shorelines and crustal deformation, San Diego to Santa Barbara, California. In: Abbott PL (ed) Geological excursions in the southern California area. San Diego State Univ, Dep Geol Sci, pp 3–15

Lajoie KR, Sarna-Wojcicki AM, Yerkes RF (1982) Quaternary chronology and rates of crustal deformation in the Ventura area, California. In: Copper JW (ed) Neotectonics in Southern California. Guideb Prep 78th Annu Meet Cordilleran Sect Geol Soc Am, pp 43–51

Lensen GJ (1968) Analysis of progressive fault displacement during downcutting at the Branch River terraces, South Island, New Zealand. Geol Soc Am Bull 79:545–556

Lensen GJ, Vella P (1971) The Waiohine River faulted terrace sequence: Recent crustal movements. R Soc N Z Bull 9:117–119

Mangerud J, Gulliksen S (1975) Apparent radiocarbon ages of recent marine shells from Norway, Spitsbergen and Arctic Canada. Quat Res 5:263–274

Matsuda T, Ota Y, Ardo M, Yonekura N (1978) Fault mechanism and recurrence time of major earthquakes in southern Kanto district, Japan, as deduced from coastal terrace data. Geol Soc Am Bull 89: 1610–1618

Meixner RE, Singer MJ (1981) Use of a field morphology rating system to evaluate soil formation and discontinuities. Soil Sci 131 (2): 114–123

Nason RE, Weertman J (1973) A dislocation theory analysis of fault creep events. J Geophys Res 78 (32):7745–7751

Nason RE, Cooper AK, Tocher D (1968) Slippage on the Buena Vista thrust fault. In: Geology and oilfields, West Side Southern San Joaquin Valley. Am Assoc Petroleum Geol, Pac Sect, pp 100–101

Olsson IU (1974) Some problems in connection with the evaluation of ^{14}C dates. Geol Foeren Stockholm Foerh 96:311–320

Olsson IU, Osadebe FAN (1974) Carbon isotope variations and fractionation corrections in ^{14}C dating. Boreas 3: 139–146

Packer D, Biggar N, Hee K (1975) Age dating geologic materials – A survey of techniques. Consultant Rep, Woodward-Clyde Consultants

Polach HA, Golson J (1966) Collection of specimens for radiocarbon dating and interpretation of results. Aust Inst Aborig Stud, Aust Natl Univ, Canberra, Manual No 2, 42 p

Proctor RJ, Crook RJr, McKeown MH, Moresco RL (1972) Relation of known faults to surface ruptures, 1971 San Fernando earthquake, southern California. Geol Soc Am Bull 83: 1601–1618

Putnam WC (1942) Geomorphology of the Ventura Region, California. Geol Soc Am Bull 53:691–754

Rockwell TK (1982) Style, rates and recency of deformation along the San Cayetano fault, western Transverse Ranges, California. Geol Soc Am Abstr Programs 14 (4):228

Rockwell TK, Keller EA (1980) Alluvial fan deformation along the San Cayetano fault, western Transverse Ranges, California. Geol Soc Am Abstr Programs 12 (3): 150

Rockwell TK, Keller EA, Clark MN, Johnson DL (1984) Chronology and rates of faulting of Ventura River terraces, California. Geol Soc Am Bull, in press

Rodgers DA (1975) Deformation, stress accumulation, and secondary faulting in the vicinity of the Transverse Ranges of Southern California. Unpublished PhD thesis, Brown Univ, 181 p

Runge ECA (1973) Soil development sequences and energy models. Soil Sci 115:183–193

Rust DJ (1982) Radiocarbon dates for the most recent large prehistoric earthquake and for late Holocene slip rates. San Andreas fault in part of the Transverse Ranges north of Los Angeles. Geol Soc Am Abstr Programs 14 (4):229

Savage JC, Burford RO (1970) Accumulation of tectonic strain in California. Seismol Soc Am Bull 60 (6):1877–1896

Savage JC, Prescott WH, Lisowski M, King N (1979) Deformation across Salton Trough, California, 1973–1977. J Geophys Res 84 (B6):3069–3079

Schubert C (1982) Neotectonics of Bocono fault, western Venezuela. Tectonophysics 85 205–220

Shackleton NJ, Opdyke ND (1973) Oxygen isotope and paleomagnetic stratigraphy of equatorial Pacific core V^{28-238} oxygen isotope temperatures and ice volumes on a 10^5 and 10^6 year scale. Quat Res 3:39–55

Sharp RV (1967) San Jacinto fault zone in the Peninsular ranges of southern California. Geol Soc Am Bull 78:705–730

Sharp RV (1981) Variable rates of late Quaternary strike slip on the San Jacinto fault zone, southern California. J Geophys Res 86 (B3):1754–1762

Sieh KE (1978) Prehistoric large earthquakes produced by slip on the San Andreas fault at Pallett Creek, California. J Geophys Res 83 (B8):3907–3938

Sieh KE (1981) A review of geological evidence for recurrence times of large earthquakes: Earthquake prediction – an international review. Maurice Ewing Ser 4. Am Geophys Un, pp 181–207

Simonson RW (1959) Outline of a generalized theory of soil genesis. Soil Sci Soc Am Proc 23:152–156

Stuiver M (1982) A high-precision calibration of the AD radiocarbon time scale. Radiocarbon 24 (1):1–26

Sylvester AG (1982) Precise leveling across active faults in California. In: Proceedings of the international symposium on geodetic networks and computations. Int Assoc Geodesy, Munich, Aug 31–Sept 5, 1981 pp 162–174

Sylvester AG, Smith RR (1976) Tectonic transpression and basement-controlled deformation in San Andreas fault zone, Salton Trough, California. Am Assoc Petroleum Geol Bull 60 (12):2081–2102

Thatcher W (1976) Episodic strain accumulation in southern California. Science 194:691–695

Thurber DL, Broecker WS, Blanchard RL, Potratz HA (1965) Uranium series ages of Pacific atoll coral. Science 149:55–58

Trifonov VG (1978) Late Quaternary tectonic movements of western and central Asia. Geol Soc Am Bull 89:1059–1072

Wallace RE (1977) Profiles and ages of young fault scarps, north-central Nevada. Geol Soc Am Bull 88:1267–1281

Wehmiller JF, Lajoie KR, Sarna-Wojcicki AM, Yerkes RF, Kennedy GL, Stephens TA, Kohl RF (1978) Amino-acid racemization dating of Quaternary mollusks, Pacific coast, United States. In: Zartman RE (ed) Short Pap 14th Int Conf Geochronol, Cosmochronol Isotope Geol. US Geol Surv Open File Rep 78–701, pp 445–448

Wesson RL, Helley EJ, Lajoie KR, Wentworth CM (1975) Faults and future earthquakes. In: Borcherdt RD (ed) Studies for seismic zonation of the San Francisco Bay region. US Geol Surv Prof Pap 941 A, pp A5–A30

Whitten CA (1956) Crustal movement in California and Nevada: Trans Am Geophys Un 37 (4):393–398

Whitten CA (1960) Horizontal movement in the earth's crust. J Geophys Res 65:2839–2849

Whitten CA (1971) Crustal-movement surveys and pre-earthquake strain analysis. In: The San Fernando Earthquake of Feb 9, 1971, US Geol Surv Prof Pap 733:161–162

Wilt JW (1958) Measured movement along the surface trace of an active thrust fault in the Buena Vista Hills. Seismol Soc Am Bull 48:169–176

Yang AIC, Fairh
and geophysi
ing, Wellingto
Yeats RS (1982) I
Geol Soc Am
Yeats RS, Clark
fornia. Groun
Yerkes RF, Boni
crustal unloa
Abstr Progr 1
Yoshikawa T, Ka
39–72

Yang AIC, Fairhall AW (1972) Variations of natural radiocarbon during the last 11 millenia and geophysical mechanisms for producing them. In: Proc 8th Int Conf Radio Carbon Dating, Wellington, New Zealand, pp A44–A57

Yeats RS (1982) Low-shake faults of the Ventura Avenue anticline, Ventura Basin, California. Geol Soc Am Abstr Programs 14 (4):246

Yeats RS, Clark MN, Keller EA, Rockwell TK (1981) Active fault hazard in southern California. Ground rupture versus seismic shaking. Geol Soc Am Bull 92: 189–196

Yerkes RF, Bonilla MG, Ellsworth WL, Lindh AG, Tinsley JC (1981) Reverse faulting and crustal unloading near Lompoc, northwest Transverse Ranges, California. Geol Soc Am Abstr Progr 13 (7):586

Yoshikawa T, Kaeyerka S, Ota Y (1981) The landforms of Japan. Univ Tokyo Press, Tokyo, pp 39–72